

Overlapping species boundaries and hybridization within the *Montastraea* “*annularis*” reef coral complex in the Pleistocene of the Bahama Islands

Ann F. Budd and John M. Pandolfi

Abstract.—Recent molecular analyses indicate that many reef coral species belong to hybridizing species complexes or “syngameons.” Such complexes consist of numerous genetically distinct species or lineages, which periodically split and/or fuse as they extend through time. During splitting and fusion, morphologic intermediates form and species overlap. Here we focus on processes associated with lineage fusion, specifically introgressive hybridization, and the recognition of such hybridization in the fossil record. Our approach involves comparing patterns of ecologic and morphologic overlap in genetically characterized modern species with fossil representatives of the same or closely related species. We similarly consider the long-term consequences of past hybridization on the structure of modern-day species boundaries.

Our study involves the species complex *Montastraea annularis* s.l. and is based in the Bahamas, where, unlike other Caribbean locations, two of the three members of the complex today are not genetically distinct. We measured and collected colonies along linear transects across Pleistocene reef terraces of last interglacial age (approximately 125 Ka) on the islands of San Salvador, Andros, and Great Inagua. We performed quantitative ecologic and morphologic analyses of the fossil data, and compared patterns of overlap among species with data from modern localities where species are and are not genetically distinct.

Ecologic and morphologic analyses reveal “moderate” overlap (>10%, but statistically significant differences) and sometimes “high” overlap (no statistically significant differences) among Pleistocene growth forms (= “species”). Ecologic analyses show that three species (massive, columnar, organ-pipe) co-occurred. Although organ-pipes had higher abundances in patch reef environments, columnar and massive species exhibited broad, completely overlapping distributions and had abundances that were not related to reef environment. For morphometric analyses, we used multivariate discriminant analysis on landmark data and linear measurements. The results show that columnar species overlap “moderately” with organ-pipe and massive species. Comparisons with genetically characterized colonies from Panama show that the Pleistocene Bahamas species have intermediate morphologies, and that the observed “moderate” overlap differs from the morphologic separation among the three modern species. In contrast, massive and columnar species from the Pleistocene of the Dominican Republic comprise distinct morphologic clusters, similar to the modern species; organ-pipe species exhibit “low” overlap (<10%, only at species margins) with columnar and massive species.

Assuming that “moderate” overlap implies hybridization and “high” overlap implies more complete lineage fusion, these results support the hypothesis of hybridization among species within the complex in the Bahamas during the Pleistocene. Hybridization involved introgression of three distinct evolutionary lineages, in association with Pleistocene sea level and temperature fluctuations, and appears to have been limited geographically primarily to the Bahamas and the northern Caribbean. Thus, not only does the structure of species boundaries within the complex vary geographically, but these geographic differences may have persisted since the Pleistocene.

Ann F. Budd. Department of Geoscience, University of Iowa, Iowa City, Iowa 52242. E-mail: ann-budd@uiowa.edu

John M. Pandolfi.* Department of Paleobiology, MRC 121, National Museum of Natural History, Smithsonian Institution, Washington D.C. 20560-0121. E-mail: Pandolfi.John@NMNH.SI.EDU

*Present address: Centre for Marine Studies and Department of Earth Sciences, University of Queensland, Brisbane, Queensland 4072, Australia

Accepted: 14 January 2004

Introduction

Understanding how species boundaries form and maintain their integrity over geologic time is fundamental to understanding the high biodiversity of tropical coral reef ecosystems. This is particularly true of reef-building

corals, many of which live sympatrically and are broadcast spawners, thereby increasing the potential for interspecific hybridization and reticulate evolution (Veron 1995). For example, in Caribbean *Acropora*, Van Oppen et al. (2000) and Vollmer and Palumbi (2002)

have recently discovered that one "species" (*A. prolifera*), which possesses a unique colony morphology, is actually a hybrid, thus adding to short-term estimates of reef diversity. However, *A. prolifera* is sterile, reproducing only by fragmentation. It therefore has no evolutionary potential and contributes little genetically to the long-term development and maintenance of reef diversity.

In contrast, similar molecular analyses of Indo-Pacific *Acropora* (Odorico and Miller 1997; Hatta et al. 1999; van Oppen et al. 2001, 2002) suggest that many species of the genus belong to hybridizing species complexes or "syngameons," in which introgressive hybridization has enhanced additive genetic variation and contributed to the generation of extraordinary species diversity. Although syngameons are composed of genetically distinct lineages (Marquez et al. 2002), morphologic "species" do not always correspond with genetic units; instead, differences in spawning times are responsible for reproductive barriers. Still other studies have shown that hybridization has led to homogenization of gene pools, reducing diversity in certain geographic areas. Two examples are *Platygyra* (Miller and Benzie 1997) and the *Montastraea* "annularis" complex (Szmant et al. 1997; Fukami et al. 2004). The latter results, in addition to those of Rodriguez-Lanetty and Hoegh-Guldberg (2002) on *Plesiastrea versipora*, suggest that geography plays an important role in the cohesiveness of species and the structure of species boundaries. Species complexes may be structured differently in different geographic areas, because genetic variability results from the accumulation of historical events over thousands of years (Benzie 1999).

One important, yet unexplored avenue in this research involves the study of species boundaries over tens to hundreds of thousands of years, and how they change through space and time. In this paper, we characterize species boundaries within one syngameon and test for hybridization in the fossil record. In our analyses, we follow Harrison's (1990) definition of hybridization as interbreeding of individuals from populations that are distinguishable on the basis of one or more heritable characters. We focus in particular on intro-

gressive hybridization, which results in incorporation of genes from one species into the gene pool of another. To recognize such hybridization in the fossil record, we compare patterns of morphologic overlap and distinctiveness in fossil species with those in related modern species, in which there is genetic evidence for hybridization (polymorphism). As revealed by comparisons of molecular and morphologic data in modern species (Fukami et al. 2004), non-hybrid (pure) populations form distinct morphologic clusters in sympatry, which do not overlap and are usually separated by gaps. Hybridizing populations are morphologically intermediate between their parent species (which are distinct, as defined above) and may overlap with parent or other related hybrid populations in one or more morphologic characters. In contrast, in more complete lineage fusion, parent populations have no distinguishing characteristics.

Our analyses focus on the *Montastraea* "annularis" complex in the late Pleistocene of the Bahama Islands. The complex ecologically dominates many modern, shallow-water reefs within the Caribbean region, and has done so since Plio-Pleistocene faunal turnover at approximately 2–1.5 Ma (Knowlton and Budd 2001). By combining rigorous sampling and morphometric analyses with quantitative ecological surveys, we address the following questions:

1. How many species exist within the complex in the Bahamas region during the late Pleistocene (last interglacial age, about 125 Ka)? Do these species represent distinct morphologic clusters separated by well-defined gaps, or is there evidence for species overlap and intermediates, suggesting hybridization?
2. Are patterns of morphologic variation within or among species related to local environmental factors (and thus adaptive) or to geography?
3. Do local environmental or geographic distributions differ among species, indicating niche differentiation?
4. Are the Pleistocene Bahamian species the same as the modern species? Are they the same as species at other Pleistocene Carib-

bean locations? How does the nature of species boundaries vary in space and in time?

5. What criteria can be used to recognize hybridization in the fossil record and trace it through geologic time?

Specifically we test the recently proposed hypothesis of Fukami et al. (2004) based on molecular data that hybridization may have occurred within the complex in the Bahamas in the geologic past and an ancestral polymorphism may have been maintained within species of the complex over the past 125 Kyr. We focus in particular on recognition of hybridization in the fossil record. In our analyses, we do not attempt to quantify amounts of observed overlap because of unequal sample sizes. However, we do categorize overlap as (1) "low" (occurring only at species margins, indicating little or no hybridization), (2) "moderate" (>10%, with the overlapping populations being statistically significantly different, indicating hybridization but incomplete lineage fusion), and (3) "high" (populations are not statistically significantly different, indicating complete lineage fusion).

Our results show that species within the complex overlap at a "moderate" to "high" level in morphology and ecology in the late Pleistocene of the Bahamas. The degree of overlap is notably higher than in older Pliocene sites in Costa Rica and Panama (Budd and Klaus 2001) and contemporaneous late Pleistocene terraces in Barbados (Pandolfi et al. 2002) and in the southern Dominican Republic (Klaus and Budd 2003), where species within the complex co-occur but remain morphologically distinct or exhibit only "low" overlap at species margins. These results support the findings of recent molecular analyses, in which the lack of genetic distinctiveness observed among modern members of the complex is interpreted as having been caused by hybridization in the geologic past (Fukami et al. 2004). They contrast with the results of similar analyses in other geographic regions (Pandolfi et al. 2001, 2002), in which character displacement (morphologic distinctiveness) driven by competition is interpreted among co-occurring species within the complex. Taken

together, studies of the species complex to date support the notion of geographical differentiation in species boundaries, which existed under different environmental conditions during the Pleistocene and persist until today.

After reviewing relevant background information in the section entitled "The *Montastraea* "annularis" species complex," this paper is organized into sections entitled "Material and Methods," "Results," and "Discussion." Each of these three main sections first contains a subsection on ecology (environments and spatial distributions) followed by a subsection on morphology (morphometric analyses). In addition, the methods section begins with a subsection on "Localities and Sampling." The results section ends with a subsection on "Comparisons in Time and Space," and the discussion section ends with inferences concerning "Hybridization and Reticulate Evolution."

The *Montastraea* "annularis" Species Complex

Genetics.—The *Montastraea annularis* species complex was first recognized by Knowlton et al. (1992) and Weil and Knowlton (1994), who proposed that the widely known generalist *M. annularis* was actually a complex of at least three sympatric and morphologically similar species in shallow to mid depths of Panama: (1) *M. annularis* sensu stricto (Ellis and Solander 1786), which forms smooth columns with senescent edges; (2) *M. faveolata* (Ellis and Solander 1786), which forms smooth mounds and plates with non-senescent edges; and (3) *M. franksi* (Gregory 1895), which forms bumpy mounds and plates with non-senescent edges. The original evidence for the complex was based on covariation between colony morphology and a number of traits including allozymes, aggressive behavior, ecology, life history, symbiont distribution, and corallite morphometrics (Tomascik 1990; Knowlton et al. 1992; Van Veghel and Bak 1993; Rowan and Knowlton 1995).

Initial analyses of allozymes sampled from these populations showed that *M. faveolata* is distinguished by a nearly fixed difference at one locus as well as frequency differences at others (Knowlton et al. 1992; Van Veghel and

Bak 1993; Weil and Knowlton 1994). Subsequent study of three amplified fragment length polymorphism (AFLP) loci and the noncoding region of the mitochondrial genome has revealed that *M. faveolata* is strongly differentiated from *M. annularis* s.s. and *M. franksi* (Lopez and Knowlton 1997; Lopez et al. 1999; Fukami et al. 2004). Although no fixed or nearly fixed differences have yet been discovered between *M. annularis* s.s. and *M. franksi*, analyses at one AFLP locus and in the noncoding region of the mitochondrial genome have revealed quantitative differences.

The potential for hybridization is supported by the fact that the three species cross-fertilize in the lab (Knowlton et al. 1997). However, spawning times in *M. annularis* s.s. and *M. franksi* characteristically differ by one to two hours, a sufficient time period to prohibit natural fertilization. Although spawning times in *M. annularis* s.s. and *M. faveolata* are the same, rates of interspecific fertilization are low between *M. faveolata* and the other two species.

Morphology.—The *Montastraea* “*annularis*” complex was not discovered prior to the allozyme work of Knowlton et al. (1992), because traditional morphologic characters do not provide enough resolution to make fine distinctions among species. Species of *Montastraea* have traditionally been distinguished on the basis of corallite diameter, number of septal cycles, the relative development of different septal cycles, and the distance between corallites (Vaughan 1919). Although corallite diameter (2–3.5 mm) and number of septal cycles (three cycles or 24 septa per corallite) are effective at distinguishing the complex as a whole, initial analyses of these “characters” revealed no single diagnostic difference among species within the complex (Knowlton et al. 1992; Weil and Knowlton 1994). Analyses of variance and canonical discriminant analysis using these characters revealed statistically significant differences among species in Panama (Weil and Knowlton 1994) and Curaçao (van Veghel and Bak 1993); however, the data distributions of these characters overlapped “moderately” among species.

Recent analyses using nontraditional corallite architectural characters (Knowlton and Budd 2001; Budd and Klaus 2001; Pandolfi et

al. 2002) revealed that the three species are discrete and do not overlap. These characters include the size and shape of the costosepta (septa = radiating partitions within corallites; costae = extensions of the septal partitions beyond the wall; costoseptum = a septum + its costal extension) and the structure of the corallite wall, and are best revealed in three dimensions on colony surfaces. Morphometric analyses showed that costae are thicker and better developed in *M. franksi*, intermediate in *M. annularis* s.s., and short and thin in *M. faveolata*. Septal relief is high in *M. faveolata*, intermediate in *M. annularis* s.s., and low in *M. franksi*; and tertiary septa are least developed in *M. faveolata* (Knowlton and Budd 2001; Budd and Klaus 2001). Cluster analysis using these characters showed distinct clusters of colonies, which closely match the results of genetic analyses performed on the same material (Budd and Klaus 2001: Fig. 1).

Calical surfaces are often worn in fossil material, making 3-D measurements unfeasible. Comparisons between 3-D measurements made on colony surfaces and 2-D measurements made on transverse thin-sections using the same modern colonies (Knowlton and Budd 2001; Budd and Klaus 2001) indicated that 2-D measurements also reveal no overlap among species within the complex. However, 2-D measurements are less effective at interpreting relationships among species. In these 2-D analyses, cluster analysis dendrograms showed that 100% of 30 genetically characterized colonies (ten *M. annularis* s.s., ten *M. faveolata*, and ten *M. franksi* from the San Blas Islands of Panama) were correctly assigned to species (Budd and Klaus 2001: Fig. 4). In addition to differences in the length and width of the costae and tertiary septa, the corallite wall is formed primarily by dissepiments (parathecal) in *M. faveolata*, and by septal thickening (septothecal) in *M. annularis* s.s. and *M. franksi* (Fig. 1).

In addition to corallite characters, several nontraditional colony-level characters have been found to differ among species (Holcomb et al. 2004). They consist of linear distances and angles measured on X-radiographs of longitudinal slabs cut through colony growth axes, and are related to upward colony growth

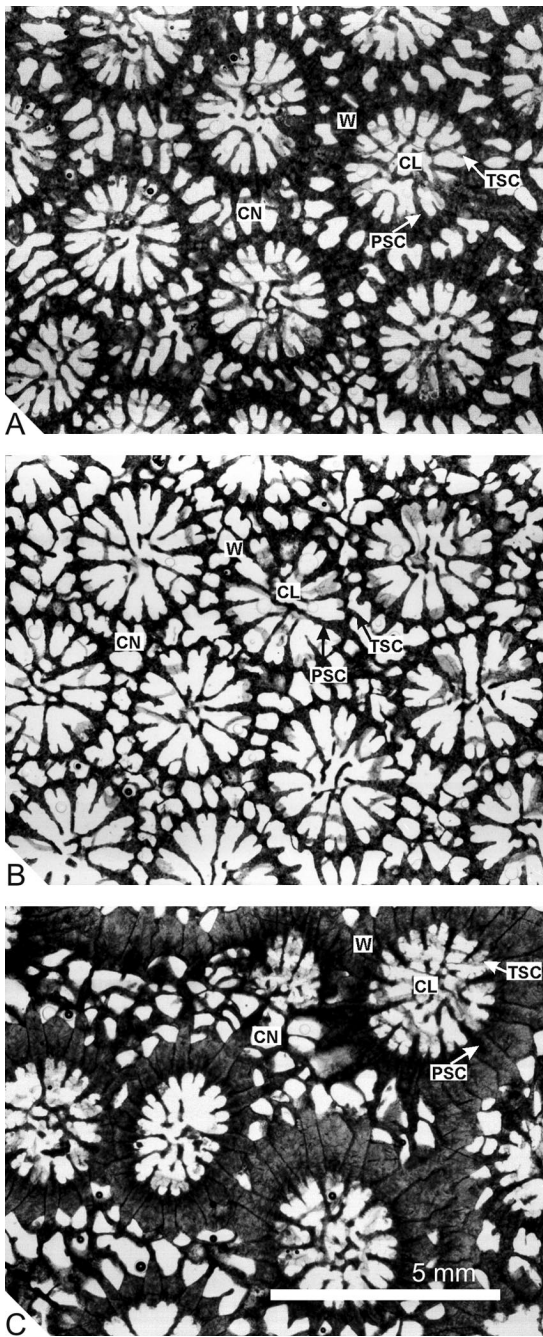


FIGURE 1. Transverse thin-sections of representative corallites of the three living species within the *Montastraea* "annularis" complex. Although corallites in the three species are similar in diameter and numbers of septa, distinct differences appear in wall structure. Corallites of *M. annularis* s.s. (A) have walls formed by septal thickening (septothecal), and well-developed extensions of costae beyond the wall. Corallites of *M. faveolata* (B) have very thin walls that are partially formed by dissepiments (parathecal); extensions of costae beyond the wall are reduced. Corallites of *M. franksi* (C) have thick septothecal walls, formed by coalesced costosepta. CL,

(extension rates), corallite budding angles, and colony curvature.

Geographic Variation and Hybridization.—Further study of living members of the complex in the Bahamas shows that the distinct boundaries among species are blurred near the northern extent of their distribution. *M. annularis* s.s. and *M. franksi* cannot be genetically distinguished in the Bahamas, and some *M. faveolata* colonies have an *M. annularis* s.s.-like genome (Fukami et al. 2004). Colony morphologies of the three species intergrade (Szmant et al. 1997). For example, *M. annularis* s.s. does not exhibit a consistent columnar morphology; its colonies range from columns to massives to plates (N. Knowlton personal observation 2000). Moreover, morphometric analyses showed corallite morphologies of *M. annularis* s.s. (columns) and *M. franksi* (plates) converge on that of *M. faveolata* (massives). As a result, the three modern species overlap and have intermediate morphologies (Fig. 2). The results of genetic analyses suggested that the observed overlap may have been caused by an ancestral polymorphism resulting from hybridization in the geologic past (Fukami et al. 2004). The ancestral polymorphism has been maintained in Bahamian *M. annularis* s.s., but lost in the other two modern species within the complex. No genetic evidence has been found for modern-day gene introgression or hybridization (Fukami et al. 2004), as has been observed in Pacific *Acropora* and is believed responsible for explosive species diversification within *Acropora* since the Pleistocene (Odorico and Miller 1997; Hatta et al. 1999). As indicated previously, here we examine patterns of overlap in the fossil record to test for the hypothesized hybridization in the geologic past.

Occurrences in the Fossil Record.—Morphometric analyses of Plio-Pleistocene fossil sequences in Costa Rica and Panama using 2-D transverse thin-section data indicated that the three modern members of the *M. "annularis"* complex originated during Plio-Pleistocene

←
columella; CN, coenosteum; PCS, primary costoseptum; TCS, tertiary costoseptum; W, wall. A, *M. annularis* s.s. (SUI 95206, a95-39); B, *M. faveolata* (SUI 95214, f95-16); C, *M. franksi* (SUI 95228, k97-1).

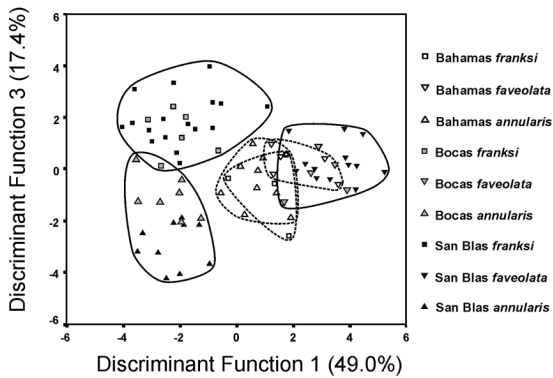


FIGURE 2. Canonical discriminant analysis of three-dimensional landmark data on genetically characterized samples of the three modern species from Panama (Bocas, San Blas) and from the Bahamas (after Fukami et al. 2004: Fig. 5). Each point on the plot represents one colony. Solid polygons enclose colonies of the same species from Panama; dotted polygons enclose colonies of the same species from the Bahamas. The first three discriminant functions in the analysis were statistically significant; functions one and three maximize the differences between the Panamanian species. Relative development of major vs. minor costae and septum height are strongly correlated with function one; costa length, minor septum length, and wall thickness are inversely correlated with function three.

turnover before the high extinction peak in Caribbean corals 2–1.5 million years ago (Fig. 3) (Budd and Johnson 1999; Budd and Klaus 2001). Two of the three modern species (*M. franksi*, *M. faveolata*) first appeared in the fossil record 3–4 million years ago and have been morphologically distinct in the central and southern Caribbean throughout their duration. Two to three undescribed fossil species were closely related to each of the two modern species, suggesting that the modern species are survivors of previously more diverse clades. The most likely ancestor of the two clades occurred in the Dominican Republic 4.5–5.5 million years ago and was morphologically similar to *M. franksi* (Budd and Klaus 2001). The third modern species (*M. annularis* s.s.) does not appear in the fossil record until about 500 Ka, and it is more closely related to *M. franksi* than to *M. faveolata* (Pandolfi et al. 2002).

Studies of coastal terraces in Barbados (Pandolfi et al. 2002), Curaçao (Pandolfi and Jackson 2001), and the southern Dominican Republic (Klaus and Budd 2003) indicated that the three modern species within the complex

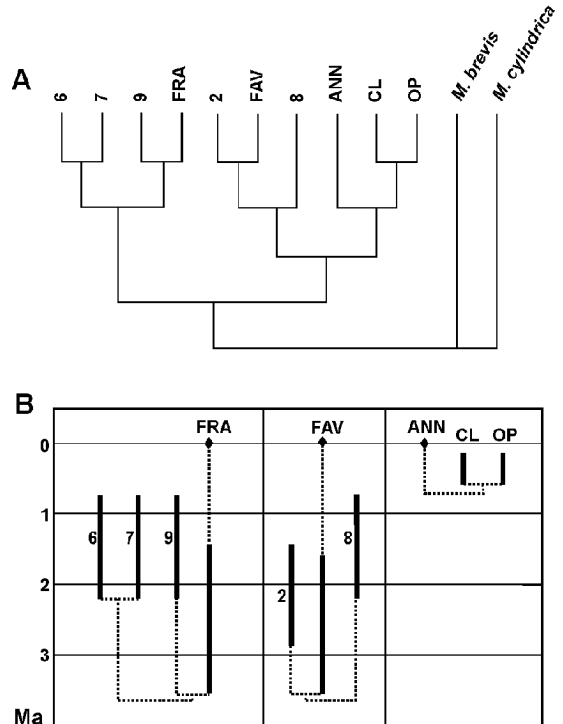


FIGURE 3. Cladogram (A) and phylogenetic tree (B) constructed for species within the *M. "annularis"* species complex (after Pandolfi et al. 2002: Fig. 1). Thick vertical lines for each species represent documented stratigraphic ranges; dotted lines represent relationships inferred from the cladistic analysis. Numbers refer to fossil Costa Rican and Panamanian species distinguished in Budd and Klaus 2001; CL and OP refer to fossil Barbados species in Pandolfi et al. 2002; ANN, modern Panamanian *M. annularis* s.s.; FRA, modern Panamanian *M. franksi*; FAV, modern Panamanian *M. faveolata*. See Pandolfi et al. 2002 for analytical details.

coexisted with one another and at least one other species (organ-pipe *Montastraea*, described in Pandolfi et al. 2001) at scattered Caribbean locations during late Pleistocene time. Although the local ecologic distributions of the four species overlapped, different species within the complex had peak abundances in different reef environments in Curaçao (Pandolfi and Jackson 2001) and Barbados (Pandolfi et al. 2001, 2002). Colony and corallite morphologies were distinct in the four species at each geographic location, and variation within species was constrained in sympatry (Pandolfi et al. 2002). After extinction of the organ-pipe species in the latest Pleistocene to early Holocene, the colony morphology of *M. annularis* s.s. shifted from thick to thin col-

TABLE 1. Summary of transects used in collecting samples and environmental and ecologic data. Statistical comparisons among islands and environments were performed with the Kruskal-Wallis H -test. For environments, 1 = reef crest, 2 = patch reef, 3 = forereef.

Transect	Envi- ron- ment	Island	Location	Collections			
				Total no. analyzed colonies	Col- umn	Mound	Organ- pipe
BP99-3w, 4m	2	San Salvador	Sue Point-no	4	0	2	2
BP99-5w, 6m	2	San Salvador	Sue Point-so	2	1	0	1
BP99-7w, 8m	2	San Salvador	Cockburn Town-so	2	1	0	1
BP99-9w, 10m	2	San Salvador	Cockburn Town-no	11	4	0	7
BP99-11w, 12m	3	Andros	Rat Cay	3	2	0	1
BP99-13w, 14m	3	Andros	Nicholls Town	3	2	1	0
BP99-15w, 16m	1	Great Inagua	north Devil's Point	16	10	4	2
BP99-17w, 18m	2	Great Inagua	north Devil's Point	14	6	1	7
BP99-19w, 20m	1	Great Inagua	north Devil's Point	4	3	0	1
BP99-21w, 22m	1	Great Inagua	north Devil's Point	13	9	1	3
BP99-23w, 24m	1	Great Inagua	west Devil's Point	12	8	2	2
BP99-25w, 26m	2	Great Inagua	west Devil's Point	22	11	3	8
TOTAL				106	57	14	35
Comparisons among islands						Chi-square	
						df	
						p -value	

umns, indicating character release following removal of ecologically similar species and corresponding to change in ecologic dominance patterns within the complex (Pandolfi et al. 2001, 2002).

Material and Methods

Localities and Sampling.—A total of 106 colonies of *M. "annularis"*-like corals (Appendix 1) were collected and morphometrically analyzed along 12 transects across well-preserved late Pleistocene terrace exposures on three Bahama Islands: (1) San Salvador, four transects, 19 colonies; (2) Andros, two transects, 6 colonies; (3) Great Inagua, six transects, 81 colonies (Table 1, Fig. 4). Uranium-thorium dating has indicated that exposures at all three locations were deposited between 132 and 118 Ka during the Sangamon sea-level highstand (White 1989; Chen et al. 1991). The three islands contain exposures of two leeward (San Salvador, Great Inagua) reef systems and one windward (Andros) reef system, which occur on widely separated and discrete carbonate platforms across the island complex. The sequences at San Salvador (Curran and White 1984, 1985; White 1989) and Great Inagua (White and Curran 1995) have been mapped and interpreted as shallowing-upward facies,

terminated by burial during sea regression (White and Curran 1987; Chen et al. 1991).

On San Salvador, two 40-m transects were measured along the terrace surface at Sue Point (White 1989), and two 40-m transects were measured at Cockburn Town (Curran and White 1984, 1985; Chen et al. 1991). At Sue Point, White (1989) has described and interpreted the exposure as representing "*Montastraea-Diploria-Porites*" patch reefs and as generally containing less *Acropora palmata* than at Cockburn Town. The entire exposure is interpreted as stratigraphically younger (about 122 Ka) than the brief sea-level lowstand at approximately 125 ka or substage 5e (Chen et al. 1991; White et al. 1998). One of our Sue Point transects was located on the north side of the previously mapped exposure (Map 1 of White 1989), and the other was measured on the south side (Map 2 of White 1989); both were measured within 5–10 m of the present shoreline.

At Cockburn Town on San Salvador, the two transects were located at the southeast end of the outcrop (i.e., southeast of "Ophiomorpha Bay") in coral rubblestone stratigraphically below and older (about 127–128 Ka) than the erosional surface interpreted as a brief sea-level lowstand at roughly 125 Ka (Chen et al.

TABLE 1. Extended.

Transects						
No. of species	<i>A. palmata</i> %	<i>A. cervicornis</i> %	<i>M. annularis</i> % complex	Total no. of colonies along transect	% Upright colonies	% Whole colonies
5	23.81	0.00	54.57	37	67.57	75.68
10	3.44	4.53	65.07	33	62.50	71.88
10	0.50	16.38	71.00	33	83.87	83.87
9	1.40	20.56	70.50	69	55.88	58.82
7	0.00	71.99	18.10	54	48.15	50.00
7	0.00	80.97	5.44	50	34.00	38.00
11	15.21	20.57	15.18	98	40.82	40.82
13	17.03	14.55	46.63	112	37.23	29.79
7	34.46	2.23	20.03	48	39.58	43.75
9	62.81	2.89	15.85	87	39.02	43.90
12	22.93	38.50	23.15	74	31.08	28.38
5	0.00	0.36	95.00	30	93.10	93.10
<hr/>						
1.478	4.479	4.647	5.436	2.605	4.205	4.154
2	2	2	2	2	2	2
0.477	0.106	0.098	0.066	0.272	0.122	0.125

1991; White et al. 1998; Wilson et al. 1998). One transect was measured on the limited exposure south of the old town public dock, and the second immediately north of the dock. The main part of the Cockburn Town reef has been characterized as "bank/barrier reef," or more specifically "fossil reef crest zone, [which] consists of near in situ *Acropora palmata* and subordinate *A. cervicornis*" (Curran and White 1984: 71). However, the portion that we transected has been interpreted as representing "Montastraea-Diploria-Porites" patch reefs (Curran and White 1984, 1985) similar to those at Sue Point.

On Andros, one 40-m transect was measured at Rat Cay, and a second was measured along the old dock on the southeast shoreline at Nicholls Town. The Nicholls Town exposure is dated as approximately 120–128 Ka (Neumann and Moore 1975), and it is composed of well-preserved, in situ colonies of *A. cervicornis*, *Diploria*, *Montastraea*, and *Porites* (Tomb 1995). No previous work has been published on the exposures at Rat Cay, but the facies and their geologic age are believed to be similar to those at Nicholls Town (M. Boardman personal observation 1999).

On Great Inagua, four 40-m transects were measured on the north side of Devil's Point

(Chen et al. 1991: Fig. 3a), and two were measured on the west side of Devil's Point (Chen et al. 1991: Fig. 3b). The transects were located stratigraphically above and in sediments younger (about 124 Ka north side and 122 Ka west side) than the brief lowstand erosion surface at roughly 125 Ka, and within 5–10 m of the present shoreline in deposits indicated as "reef 2" by Chen et al. (1991). The north-side transects were placed in "coral rubblestone" containing well-preserved, in situ colonies of the genera *Acropora*, *Diploria*, *Montastraea*, and *Porites* and interpreted as "bank/barrier reef" by White and Curran (1987, 1995). The west-side transects were placed in the "in situ patch reef," composed of *Porites* and *Montastraea* (Chen et al. 1991).

Each of the twelve 40-m transects was laid parallel to the shoreline through a well-preserved portion of each exposure. We collected fist-sized samples (106 total; Appendix 1) from representative well-preserved colonies along each transect for detailed morphometric analysis. The samples were shipped to Iowa, and one transverse thin-section and one 7-mm-thick vertical slab were prepared from each sample. The samples will be deposited at the National Museum of Natural History (Appendix 1).

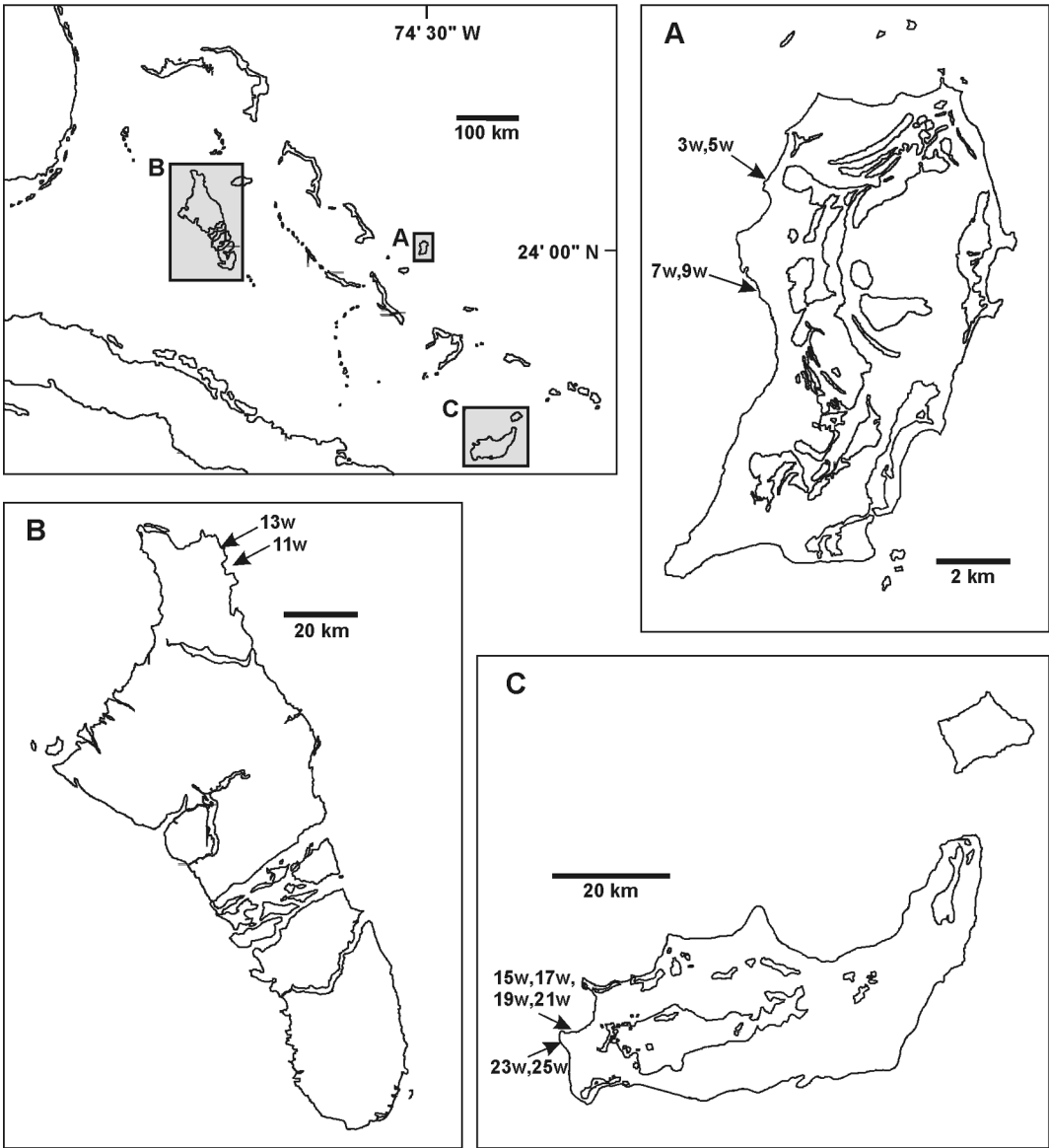


FIGURE 4. Maps showing locations of the 12 transects (Table 1). All transects were laid across late Pleistocene coastal terraces, dating between 132 and 118 Ka. A, San Salvador, transects 3w, 5w, 7w, 9w; B, Andros, transects 11w, 13w; C, Great Inagua, transects 15w, 17w, 19w, 21w, 23w, 25w.

Environments and Spatial Distributions.—Two different types of data were recorded along each transect (Appendix 2): (1) whole-community data (odd-numbered transects with the suffix “w”), used in environmental interpretations, and (2) *Montastraea*-only data (even-numbered transects with the suffix “m”), used in characterizing the spatial distributions of different growth forms within the complex.

(1) *Whole-community data:* Using the methods of Pandolfi (2001) and Pandolfi and Jackson (2001), we recorded the intercept lengths of all corals that crossed each transect line. Individual colonies were distinguished and identified to species (19 total, including the *M. annularis* complex as a single species; Appendix 2). Following the approach of Knowlton et al. (1992), Weil and Knowlton (1994), and Pandolfi et al. (2001), we identified mem-

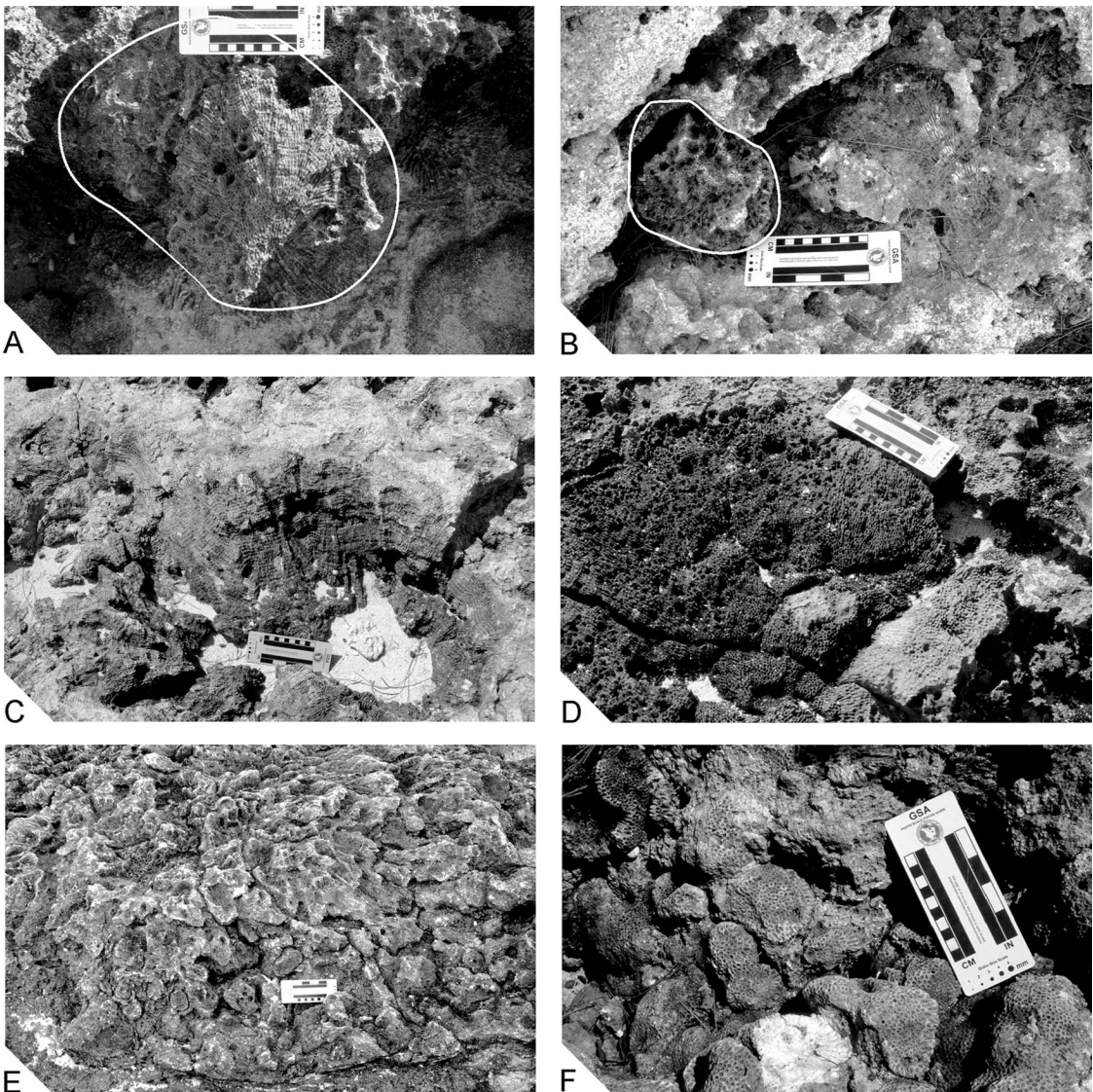


FIGURE 5. Field photos showing different growth forms of the *M. "annularis"* complex. Columns are circled in white. A, Columnar form, transect 15w, North Devil's Point, Great Inagua. B, Columnar form, transect 9w, Cockburn Town (north), San Salvador. C, Massive form, transect 9w, Cockburn Town (north), San Salvador. D, Massive form, transect 5w, Sue Point (south), San Salvador. E, Organ-pipe form, transect 19w, North Devil's Point, Great Inagua. F, Organ-pipe form, transect 3w, Sue Point (south), San Salvador.

bers of the *M. "annularis"* complex in the field by growth form (organ-pipe, column, massive, plate). *Organ-pipe* colonies were qualitatively defined as composed of numerous elongate skeletal pipes whose diameters were usually less than 10 cm thick; *columnar* colonies as composed of multiple skeletal columns (higher than wide) with diameters usually 10–35 cm thick; *massive* colonies as composed of a usually single mound-shaped skeletal mass

with a diameter >35 cm thick (Fig. 5) (Pandolfi et al. 2001); and *platy* colonies as composed of elongate, thin plates (<25 cm high). Orientation (upright vs. overturned) and breakage (whole vs. fragment) were also recorded for each colony.

(2) *Montastraea-only* data: We recorded every *M. "annularis"*-like colony that occurred within 0.5 m of the transect line, and its diameter, orientation, and breakage. The colonies were

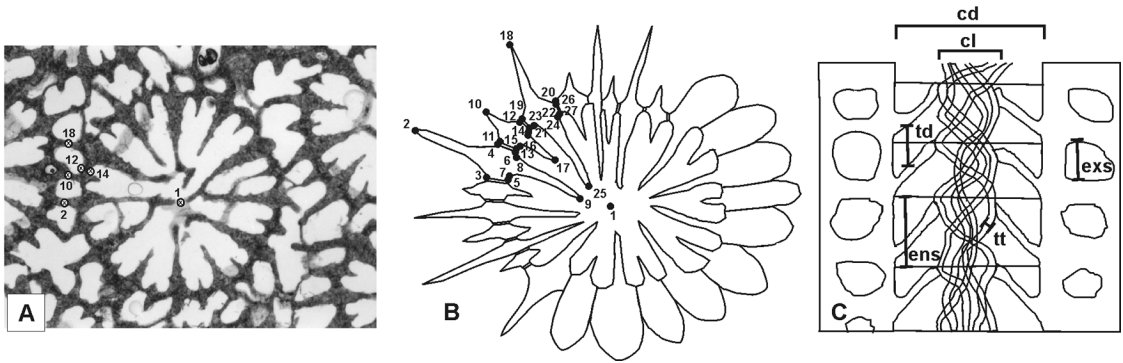


FIGURE 6. A, B, Transverse thin-sections. Two-dimensional Cartesian coordinates collected for 27 landmarks; only extremal landmarks are shown. The landmarks consist of spatially homologous points designed to reflect the structure of the corallite wall and costal extensions beyond the wall. Points 1 and 14 and points 1 and 12 served as baselines in calculating shape coordinates. C, Longitudinal slabs. Five linear distances were measured: cd, corallite diameter; cl, columella width; td, vertical distance between columella threads; tt, thickness of columella thread; ens, distance between endothelial dissepiments; exs, distance between exothelial dissepiments. Five measures were made per corallite; three corallites were measured per colony.

identified by growth form (organ-pipe, column, massive, plate) as defined above.

Data on the species richness, dominant coral species (% *Acropora palmata*, % *A. cervicornis*, % *M. "annularis"* complex), and coral orientation and breakage are summarized for each transect in Table 1. For preliminary comparisons of these data among islands and among interpreted reef environments, we used non-parametric tests comparing independent samples (Kruskal-Wallis *H*; SPSS 11.0).

We performed multidimensional scaling analysis of the whole community data, in which growth forms of the *M. "annularis"* complex were lumped into one taxon. Using the same procedures we analyzed the *Montastraea*-only transect data to characterize the spatial distributions of the three Pleistocene growth forms. In these analyses, we used the Bray-Curtis dissimilarity coefficient (Bray and Curtis 1957) to compare taxonomic composition among all possible pairs of transects. Dissimilarity values range from 0 (for a pair of samples with identical taxonomic composition) to 1 (for a pair of samples with no taxa in common). Abundance data were transformed to their square roots before the calculation to reduce the influence of occasional large abundance values for some taxa (Field et al. 1982). The transformed abundance values for each taxon were standardized by the maximum attained by that taxon. This standardi-

zation equalizes the potential contributions of taxa to the overall dissimilarity in composition. Without standardization by taxon, the Bray-Curtis values are dominated by those taxa that attain high abundances (Faith et al. 1987). We used global non-metric multidimensional scaling as an ordination technique to provide a visual summary of the pattern of Bray-Curtis values among the samples. Calculation of dissimilarity matrices and ordinations were performed with the PRIMER software package. Details of these methods can be found in the studies by Pandolfi and Minchin (1995), Pandolfi (1996), Jackson et al. (1996), Pandolfi (2001), and Pandolfi and Jackson (2001).

Morphometric Analyses.—Data were collected on transverse thin-sections and longitudinal slabs within each of the 106 colonies. We used the 2-D approach on transverse thin-sections (described above) in our study because colony surfaces were weathered, making the 3-D approach unfeasible. We obtained Cartesian coordinates (x-y) for 27 landmarks on six corallites in transverse thin-sections (Fig. 6, Appendix 3). This same approach has been applied in studies of the complex in the late Pleistocene of Barbados (Pandolfi et al. 2002), the Plio-Pleistocene of Costa Rica and Panama (Budd and Klaus 2001), and the late Miocene and late Pleistocene of the Dominican Republic (Klaus and Budd 2003).

TABLE 2. List of transverse and longitudinal characters analyzed. Shape coordinates (x1. . .x25, y11. . .y22) were selected, if they defined single morphologic structures and did not combine several different structures into one variable. Numbers for Tukey's test refer to Pleistocene Bahamian growth forms (1 = columnar, 2 = massive, 3 = organ-pipe) and modern Panamanian members of the *M. "annularis"* complex (4 = *M. annularis* s.s., 5 = *M. faveolata*, 6 = *M. franksi*). Species may belong to two groups (= homogeneous sets of means, in brackets) if there is partial overlap among groups. ns = not significant.

Shape coordinates, centroid size, and linear measurements	Character definition	Tukey's HSD multiple comparisons test
<i>Transverse</i>		
x18, baseline = 1,12	extension of primary costa	[6=(3=2)] < [(3=2)=(1=5)] < [(1=5)=4]
x2, baseline = 1,12	extension of secondary costa	[6=3] < [3=(2=1=4)] < [(2=1=4)=5]
x10, baseline = 1,12	extension of tertiary costa	[6=(2=3)] < [(2=3)=(1=5)] < [3=(1=5)=4]
x25, baseline = 1,14	length of primary septum	*ns
x9, baseline = 1,14	length of secondary septum	*ns
x17, baseline = 1,14	length of tertiary septum	*ns
x14, baseline = 1,12	wall thickness	[6] < [3=1=4=2] < [5]
x21, baseline = 1,12	wall thickness	[6] < [3=1=4=2] < [5]
y19, baseline = 1,12	outer length of wall dissepiment	[6=3=5=(1=4)] < [(1=4)=2]
y21, baseline = 1,14	inner length of wall dissepiment	[6=(3=5)] < [(3=5)=(1=4)] < [5=(1=4)=2]
y11, baseline = 1,12	outer width of tertiary wall costoseptum	[6] < [3=1=4=5=2]
y22, baseline = 1,14	inner width of primary wall costoseptum (plus dissepiment)	*ns
x16, baseline = 1,14	width of tertiary septum	[2=6=3=(4=1)] < [(4=1)=5]
LENGTH, baseline = 1,14	corallite diameter	[4=(3=1=6)] < [(3=1=6)=5=2]
CSIZE	centroid size (all 27 landmarks)	[4=(5=1)] < [(5=1)=3=2<6]
<i>Longitudinal</i>		
cd	corallite diameter	*[3=1] < [1=2]
cl	columella thickness	*ns
td	vertical distance between columella threads	*ns
tt	thickness of columella threads	*ns
ens	distance between endothecal dissepiments	*[1=3] < [2]
exs	distance between endothecal dissepiments	*ns

* Pleistocene only.

In an effort to improve resolution in distinguishing species, we added measurements related to colony growth to the transverse thin-section data set. This step was not taken in previous work. Colony growth within the complex involves three different growth processes: (1) upward skeletal extension, (2) calcification or skeletal thickening, and (3) bud-

ding of new corallites within colonies (Graus and Macintyre 1982). Morphologic features resulting from these processes are best observed in longitudinal slabs and thin-sections. We measured six features on longitudinal slabs that were cut along the growth axis of each colony (Table 2, Fig. 6).

Size and shape coordinates (Bookstein

1991) were calculated for landmark data by using the computer program GRF-ND (generalized rotational fitting of n-dimensional landmark data, 1994, written by Dennis E. Slice available at <http://life.bio.sunysb.edu/morph/>). Centroid size was calculated by summing the squared distances from each of the 27 landmarks to a common centroid. To calculate shape coordinates we used triplets of the 27 points. Different sets of shape coordinates were calculated separately by using two baselines: (1) points 1 to 14 and (2) points 1 to 12. To facilitate morphologic interpretation, we selected 13 shape coordinates associated with the structure and development of the corallite wall and costosepta (Table 2) for use in statistical analyses.

To test whether the Pleistocene column, massive, and organ-pipe growth forms represented different species, we performed canonical discriminant analyses [SPSS 11.0] using the 15 transverse and six longitudinal characters as variables (Table 2) and the three growth forms as groups (the platy form was not sampled). To test whether the colonies from different environments within the three growth forms differed in morphology, we performed canonical discriminant analyses using the same 15 transverse and 6 longitudinal characters as variables (Table 2). We also performed univariate comparisons of means among growth forms and among environments within each growth form using multiple comparisons tests (Tukey's HSD).

To test whether the three Pleistocene Bahamian growth forms are the same as the modern members of the *M. "annularis"* complex, we compared them with data collected in the same manner on transverse thin-sections of 30 genetically characterized modern colonies, consisting of ten *M. annularis* s.s. (columns), ten *M. faveolata* (massives), and ten *M. franksi* (plates) from a shallow forereef environment in the San Blas Islands of Panama. This modern data set is described in detail by Budd and Klaus (2001) and Fukami et al. (2004). In addition to multivariate analyses, we also performed univariate comparisons of means, using multiple comparisons tests (Tukey's HSD) to compare the three growth forms

with the modern species, and we used box-plots to examine the results.

To test whether the three Pleistocene Bahamian growth forms are the same as similar-aged growth forms of the *M. "annularis"* complex from the central Caribbean, we compared them with data collected in the same manner on transverse thin-sections of colonies from a late Pleistocene terrace (about 125 Ka) along the southern coast of the Dominican Republic. This data set is described by Klaus and Budd (2003).

Results

Environments and Spatial Distributions

Environments.—Examination of the whole community data (Table 1) shows that species richness ranged from 5–13 per transect (median = 9 species). There are no significant differences among islands in numbers of species per transect, numbers of colonies per transect, taxonomic composition, or percent upright or whole colonies per transect (Table 1). Multidimensional scaling ordination of whole community data (Fig. 7) groups the transects into three assemblages: (1) transects 15w, 19w, 21w, 23w on Great Inagua (abundant *A. palmata*); (2) transects 3w, 5w, 7w, 9w on San Salvador, and transects 17w and 25w on Great Inagua (abundant *M. "annularis"* complex); and (3) transects 11w and 13w on Andros (abundant *A. cervicornis*). These groups agree with previous findings by Curran and White (1984, 1985), White and Curran (1987), and White (1989), who interpreted the three types of exposures as respectively representing reef crest, patch reef, and forereef environments. These three "environments" form the basis of subsequent analyses of morphology and spatial distributions of growth forms within the *M. "annularis"* complex.

Spatial Distributions.—*Montastraea*-only analyses treated only data recorded on San Salvador and Great Inagua, because of the low numbers of *Montastraea* recorded on Andros. The results of multidimensional scaling analyses using *Montastraea*-only data (Fig. 8) indicate the following:

1. Massive, columnar, and organ-pipe growth

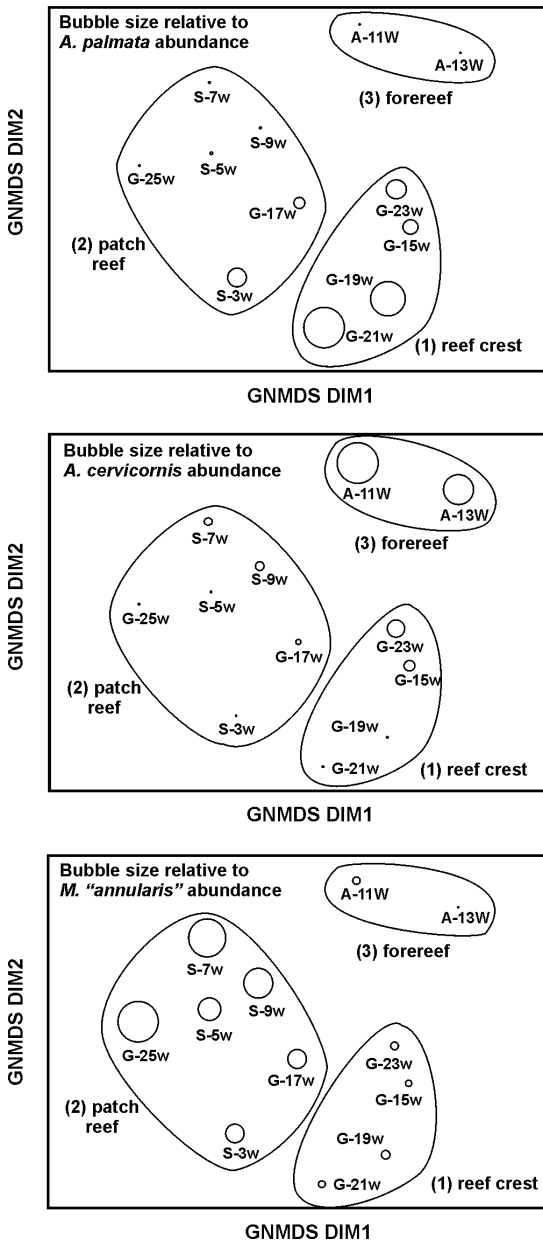


FIGURE 7. Global nonmetric multidimensional scaling (GNMDS) ordination of whole community transect data (Appendix 1) for all 12 transects. Study of plots of the first two dimensions, combined with relative abundances of *A. palmata*, *A. cervicornis*, and *M. "annularis"* sensu lato, suggests that the transects can be grouped into three assemblages corresponding with reef crest, patch reef, and forereef environments. S, San Salvador; A, Andros; G, Great Inagua.

forms co-occur in all three environments, on all two islands.

2. Organ-pipes are most abundant in the patch reef environment (lower energy), where the entire *M. "annularis"* complex is generally most abundant (Fig. 7); the abundance of organ-pipes in patch reef environments is higher than the abundances of either columns or massives.
3. The abundances of columns and massive forms are highly variable, and not related to environment or to the abundance of other growth forms; columnar forms have higher abundances than organ-pipes on the reef crest.
4. Within growth forms, differences in abundances are not related to geography, suggesting that factors limiting abundance do not vary across the Bahamian platform.

Morphology

Variation among Growth Forms.—To test whether the three growth forms represented different species, we performed canonical discriminant analyses using 21 variables (Table 2) and the three growth forms as groups. Because of previously observed high ecophenotypic plasticity within the complex (Foster 1979; Graus and Macintyre 1982; Budd 1993), we first performed the discriminant analyses separately on colonies from the reef crest (environment #1, $n = 45$ colonies) and patch reef (environment #2, $n = 55$ colonies) environments. These two environments had higher sample sizes than the forereef (environment #3), and each growth form consisted of at least six colonies (Table 1). The results of the canonical discriminant analyses (Fig. 9) show that, although the three growth forms have statistically significant differences in corallite morphology, the columnar form overlaps "moderately" with both the organ-pipe and massive growth forms. In both analyses, multiple comparisons tests (Tukey's HSD) indicate that differences between the three growth forms are statistically significant on the first discriminant function, and that the massive form differs significantly from the organ-pipe and columnar forms on the second function.

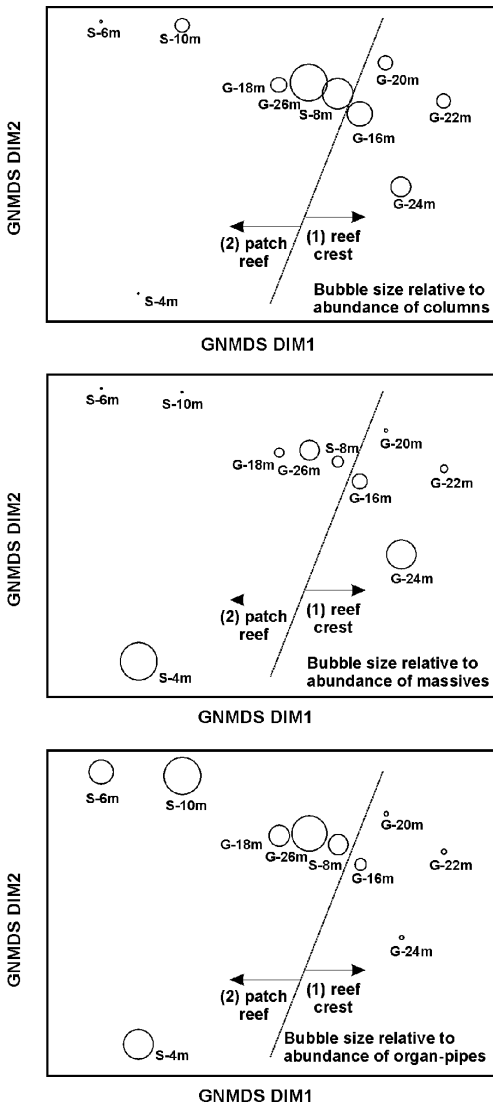


FIGURE 8. Global nonmetric multidimensional scaling (GNMDS) ordination of *Montastraea* transect data (Appendix 1) for ten transects (excluding the two transects in Andros). Study of plots of the first two dimensions, combined with relative abundances of the three growth forms, suggests that the three growth forms co-occur in reef crest and patch reef environments on both San Salvador and Great Inagua. Organ-pipes have higher abundances in patch reef environments; the abundances of columns and massives are variable. *Montastraea*-only analyses focused only on San Salvador and Great Inagua, because of the low numbers of *Montastraea* recorded on Andros; S, San Salvador; G, Great Inagua.

Moreover, massive and organ-pipe forms are clearly separated (Fig. 9A,B).

Next, using colonies from all three environments we performed an all-inclusive canonical discriminant analysis comparing the three

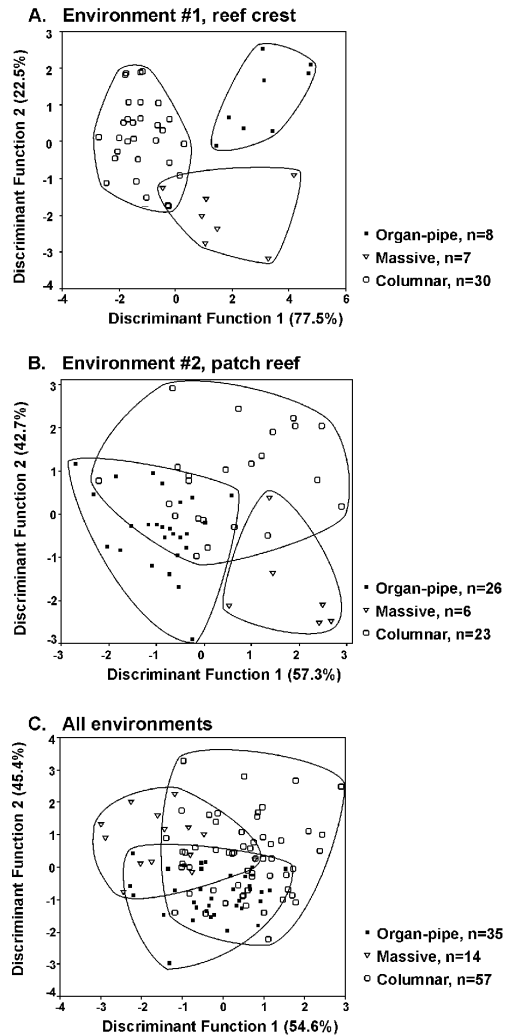


FIGURE 9. Plots of scores in canonical discriminant analyses comparing the Pleistocene growth forms. Each point on the plots represents one colony; polygons enclose growth forms. A, Analysis for environment #1 (reef crest), 93.9% correctly classified; Tukey's HSD test (using $p < 0.05$) shows that columnar < massive < organ-pipe for function 1, and massive < columnar = organ-pipe for function 2. B, Analysis for environment #2 (patch reef), 83.6% correctly classified; Tukey's HSD test (using $p < 0.05$) shows that organ-pipe < columnar < massive for function 1, and massive < organ-pipe < columnar for function 2. C, Analysis for all three environments combined, 68.9% correctly classified; Tukey's HSD test (using $p < 0.05$) shows that massive < organ-pipe < columnar for function 1, and organ-pipe < columnar = massive for function 2. Length of costal extensions (x2, x18, x10, csz), septum width (x16), and dissepiment spacing (ens) are strongly correlated with the first function in the reef crest (A) and combined analyses (C), and with the second function in the analysis of the patch reef (B). Wall thickness (x14, x21) and development of wall dissepiment (y21, y19) are strongly correlated with the second function in the reef crest (A) and combined (C) analyses, and with the first function in the patch reef (B) analysis (Appendix 4).

growth forms ($n = 106$ colonies). The results reveal significant differences, but even more overlap. Although the columnar form overlaps "moderately" with the massive and organ-pipe forms (Fig. 9C), multiple comparisons tests (Tukey's HSD) show that differences between it and the other two forms are statistically significant on the first discriminant function, but that differences between the columnar and massive forms are not significantly different on the second function. Massive and organ-pipe forms also overlapped "moderately" but to a lesser degree; they differed significantly on both the first and second functions (Fig. 9C).

As indicated by the correlation table between individual variables and canonical discriminant functions in the all-inclusive analysis (Appendix 4), the massive form is distinguished by high values along function 2 and low values along function 1, which are correlated respectively with well-developed dissepiments (y19, y21), thinner walls (x14, x21), and larger corallites (cd) (function 2), and with shorter, narrower costae (x10, x16) and widely spaced endothecal dissepiments (ens) (function 1). The organ-pipe form is distinguished by low values along function 2, which are correlated with thick wall (x14, x21) and poorly developed dissepiments (y19, y21). The columnar form encompasses the range of variation along function 2 but has higher values along function 1, indicating longer, wider costae (x10, x16). These differences are illustrated in Figure 10 and are further confirmed by multiple comparisons tests (Tukey's HSD) (Table 2).

Variation within Growth Forms.—To test whether the colonies from different environments within the three growth forms differed in morphology, we used the same 21 variables (Table 2) to perform canonical discriminant analyses comparing reef crest and patch reef environments (the two environments with adequate numbers of colonies per growth form for statistical analysis, see Table 1). Canonical discriminant analyses within massive and organ-pipe growth forms indicate that corallite morphology differs markedly between reef crest and patch reef environments; only in the columnar form do colonies from these envi-

ronments overlap in corallite morphology (Fig. 11). Moreover, multiple comparisons tests (Tukey's HSD test) show that differences between environments within all three growth forms are statistically significant.

Species diagnostic characters such as costal extensions (x2, x10, x18) and wall structure (y19) are correlated with the discriminant function in the organ-pipe growth form, which has longer costae and well-developed dissepiments in the patch reef. However, in columns and in massives different sets of variables, many of which were *not* important in distinguishing species (Table 2), are correlated with the function (Appendix 5). In these two cases, length of the tertiary septum (x17), exothecal dissepiment spacing (exs), and columella thickness (cl) are most strongly correlated with the function. In columns, the tertiary septa are better developed in environment #2 (patch reef). In massives, the columella is thicker and exothecal dissepiments are more narrowly spaced in environment #2 (patch reef). As shown in Figure 10, costal extensions are short, walls are thick, and wall dissepiment is less developed in environment #3 (forereef).

Comparisons in Time and Space

Comparison with Modern Species in the Complex.—To test whether the three Pleistocene Bahamian growth forms are the same as the modern members of the *M. "annularis"* complex, we performed a canonical discriminant analysis comparing the three Bahamian Pleistocene species with samples of the three modern species from the San Blas Islands of Panama. To minimize the effects of fossilization (diagenesis, breakage) on these comparisons, we first performed *t*-tests comparing each of the 15 transverse thin-section variables between all fossil and all modern colonies, and used the results to select 11 of the 15 variables with insignificant differences for inclusion in the discriminant analysis. The four variables that were removed (x9, x25, x17, y22) consist of measures of septal length and width, which were only weakly correlated with the previous discriminant functions distinguishing fossil species (Appendices 4, 5).

The results indicate that the modern species

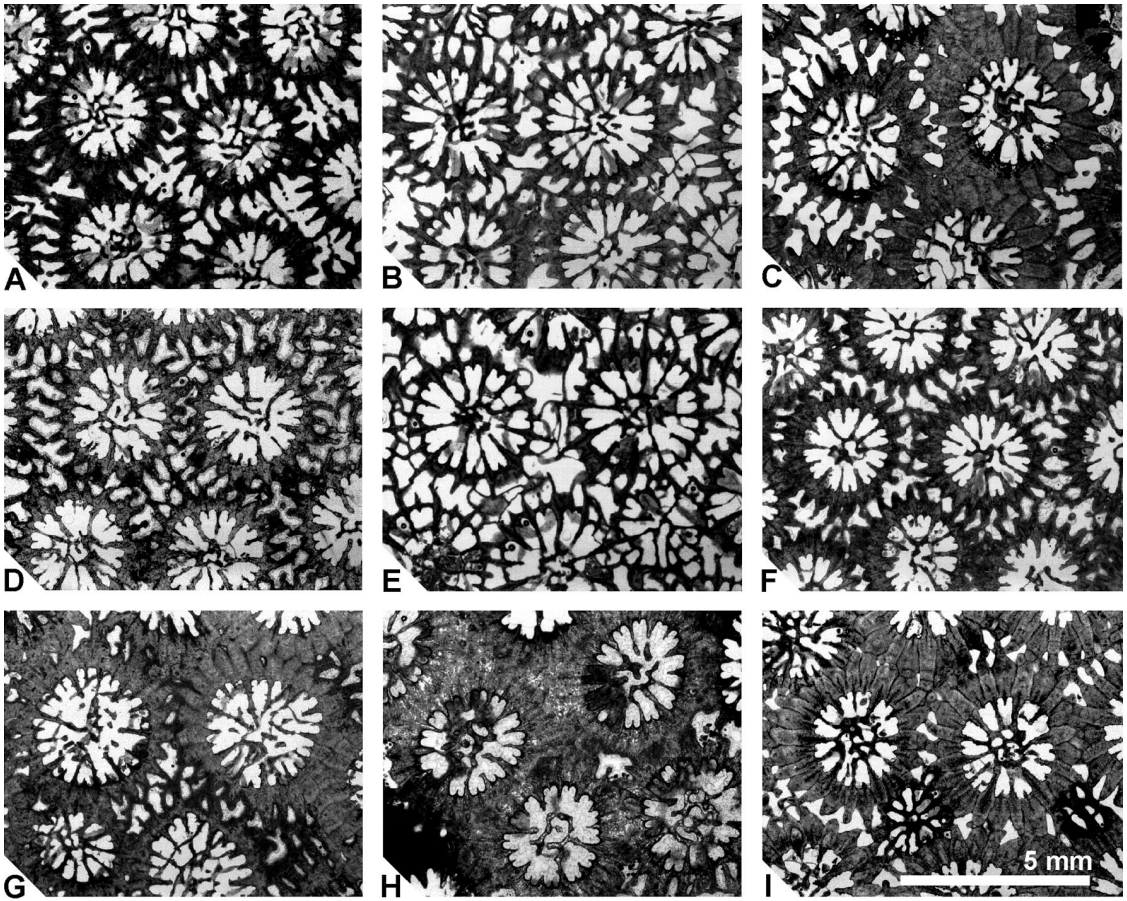


FIGURE 10. Transverse thin-sections of representative corallites of the three growth forms of the *M. "annularis"* complex collected in three different reef environments in the Pleistocene of the Bahamas. The massive form (B, E, H) is distinguished by well-developed dissepiments, thinner walls, larger corallites, and shorter, narrower costae ($\times 10$, $\times 16$); the organ-pipe form (C, F, I) is distinguished by its thick corallite wall and poorly developed dissepiments. The columnar form (A, D, G) is highly variable and has longer, wider costae. Within growth forms, costal extensions are short and corallite walls are thick in environment #3 or forereef (G, I). In columns, the tertiary septa are better developed in environment #2. In massives, the columella is thicker and exothecal dissepiments are more narrowly spaced in environment #2. In the organ-pipes, the corallite wall is distinctively septothecal in environment #1, and costal extensions are short (F). A–C. Environment #1 (reef crest). A, Columnar growth form, BPK10221. B, Massive growth form, BPK10258. C, Organ-pipe growth form, BPK10159. D–F. Environment #2 (patch reef). D, Columnar growth form, BPK10422. E, Massive growth form, BPK10151. F, Organ-pipe growth form, BPK10310. G–I. Environment #3 (forereef). G, Columnar growth form, BPK10022. H, Massive growth form, BPK10057. I, Organ-pipe growth form, BPK10045.

are widely separated and collectively occupy more morphospace than the Pleistocene species (Fig. 12). In contrast, the three Pleistocene species show "moderate" to "high" overlap. Study of patterns of overlap among the six groups using Mahalanobis distances shows that only the Pleistocene columns and *M. annularis* s.s. (columns) are not statistically significantly different ($F = 1.302$, $p = 0.274$), and overlap is "high." All other pairwise comparisons reveal significant differences. Of the

three modern species, Pleistocene massives and organ-pipes are both most similar to *M. annularis* s.s. (columns) and exhibit "moderate" overlap. The distance between *M. annularis* s.s. and Pleistocene massives is small, but significant ($F = 2.698$, $p = 0.028$); the distance between *M. annularis* s.s. and Pleistocene organ-pipes is greater ($F = 6.836$, $p < 0.001$).

These results indicate that, although the Pleistocene Bahamas and Recent Panama columns (= *M. annularis* s.s.) have similar cor-

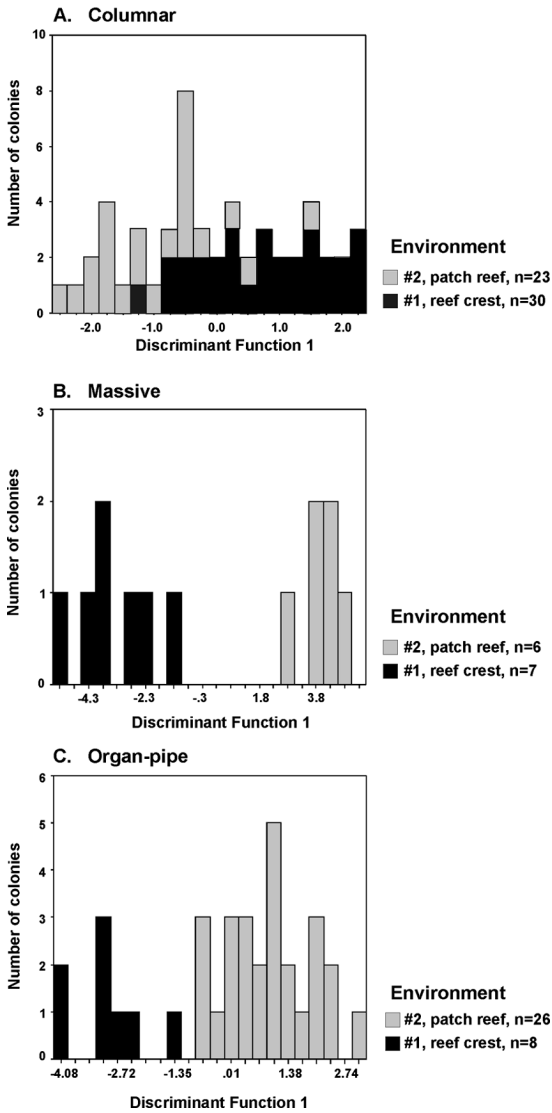


FIGURE 11. Plots of scores in canonical discriminant analysis comparing environments #1 (reef crest) and #2 (patch reef) within the Pleistocene species. A, Columnar growth form; B, Massive growth forms. C, Organ-pipe growth form.

allite morphologies and appear to represent the same species, the Pleistocene Bahamas and Recent Panama massive forms do not (Fig. 12). In fact, the Pleistocene Bahamas massives have corallite morphologies closer to the Pleistocene Bahamas columns and Recent Panama columns (= *M. annularis* s.s.), than they do to the Recent Panama massives (= *M. faveolata*).

The observed similarities and “high” overlap between the Pleistocene columns and *M.*

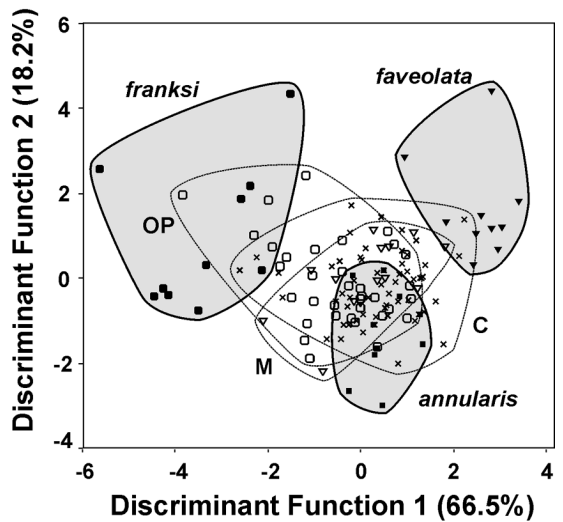


FIGURE 12. Plot of scores in a canonical discriminant analysis comparing the three Pleistocene Bahamas growth forms and the three modern species. Each point on the plot represents one colony; polygons enclose each of the six groups. C = Pleistocene columns, M = Pleistocene massive colonies, OP = Pleistocene organ-pipes. Wall thickness (x14, x21) is most strongly correlated with the first function; corallite size (csize, LENGTH), in combination with wall structure (y21, y19), is most strongly correlated with the second function. These results and the results of Tukey’s HSD test (Table 2) indicate that in the Pleistocene columns and *M. annularis* s.s., corallites are small (LENGTH), costal extensions (x18, x2, x10) are long, wall thickness (x14, x21) is intermediate, and wall dissepiment (y21, y19) is poorly developed. The Pleistocene organ-pipes differ from the latter two species in their short costal extensions. The Pleistocene massive forms are similar to *M. faveolata* (massives) in their large corallite diameter (LENGTH) and intermediate costal extensions (x18, x2, x10); however, *M. faveolata* has a distinctive thin wall (x14, x21), thin tertiary septa (x16), and less well developed wall dissepiments (y21, y19). *M. franksi* (plates) is distinguished by its short costae (x18, x2, x10), thick wall (x14, x21), and the presence of wall dissepiment (y21, y19).

annularis s.s. (columns), the “moderate” overlap among the Pleistocene species, and the distinctiveness of the three modern species are confirmed in analyses of single variables using pairwise comparisons of means (Tukey’s HSD test) (Table 2, Fig. 13).

Comparison with Pleistocene Species of the Dominican Republic.—In the final analysis, we compared the three Pleistocene Bahamian growth forms with similar-aged growth forms of the *M. “annularis”* complex from the Dominican Republic. We used data collected in the same manner on transverse thin-sections of 114 colonies, consisting of 43 columns, 14

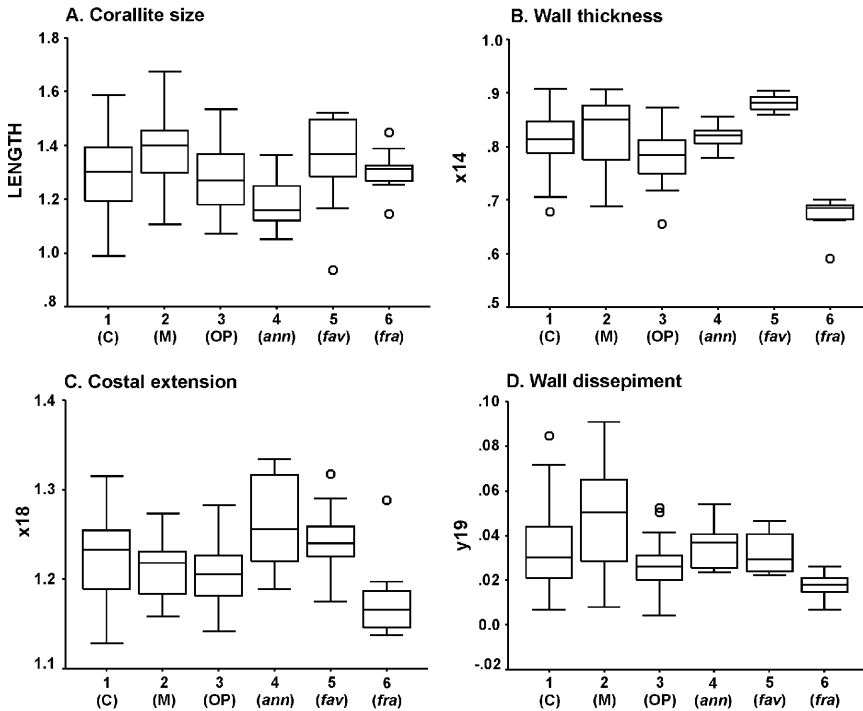


FIGURE 13. Boxplots of size and shape coordinates based on the median, quartiles, and extreme values. The selected variables represent four different patterns of morphologic variation among species. The box represents the interquartile range containing 50% of the values. The whiskers represent the highest and lowest values, excluding outliers. The line across each box represents the median. 1 = Pleistocene columns ($n = 57$), 2 = Pleistocene massive colonies ($n = 14$), 3 = Pleistocene organ-pipes ($n = 35$), 4 = modern *M. annularis* s.s. ($n = 10$); 5 = modern *M. faveolata* ($n = 10$); 6 = modern *M. franksi* ($n = 10$). Species may belong to two groups (= homogeneous sets of means), if there is partial overlap among groups. A, Baseline (1–14) length (corallite diameter), Tukey's HSD test using $p < 0.05$ (Table 2): $[4 = (3 = 1 = 6)] < [(3 = 1 = 6) = 5 = 2]$. B, x21 (wall thickness), Tukey's HSD test: $[6] < [3 = 1 = 4 = 2] < [5]$ (x14 has the same pattern). C, x18 (extension of primary costa), Tukey's HSD test: $[6 = (3 = 2)] < [(3 = 2) = (1 = 5)] < [(1 = 5) = 4]$ (x10, x2 have similar patterns; csiz has an inverse pattern). D, y21 (inner length of wall dissepiment), Tukey's HSD test: $[6 = (3 = 5)] < [(3 = 5) = (1 = 4)] < [5 = (1 = 4) = 2]$ (y19 has a similar pattern). In y11 (outer width of tertiary wall costoseptum), *M. franksi* (6) is wider than the other five groups. In x16 (width of tertiary septum), *M. faveolata* (5) is thinner than the other five groups.

massives, 5 plates, and 52 organ-pipes, from a range of back reef, reef crest, and reef front environments (Klaus and Budd 2003). We performed two canonical discriminant analyses: (1) comparing the four growth forms of the Dominican Republic, leaving the three growth forms of the Bahamas "unclassified" (i.e., not assigning them to an a priori group) (Fig. 14A), and (2) comparing the three modern species, leaving the Dominican Republic growth forms unclassified (Fig. 14B). All 15 variables were used in the first analysis; the 11 variables in the modern analyses (described above) were used in the second analysis.

The results of the discriminant analyses comparing growth forms in the Dominican Republic indicate that three of the four Do-

minican Republic growth forms exhibit overlap at species margins; overlap is "moderate" or greater between the Dominican Republic columnar and organ-pipe forms, and is "low" between organ-pipe and massive forms (Fig. 14A). In comparisons between Dominican Republic and Bahamas growth forms, the Dominican Republic growth forms form clusters (= concentrations of specimens), albeit with "low" to "moderate" overlap. The Bahamas growth forms appear haphazardly scattered and do even not form clusters (Fig. 14A); overlap is "high." Unlike the Bahamas, the Dominican Republic massives and columns do not overlap, indicating that patterns of morphologic variation are distinctively different at the two locations.

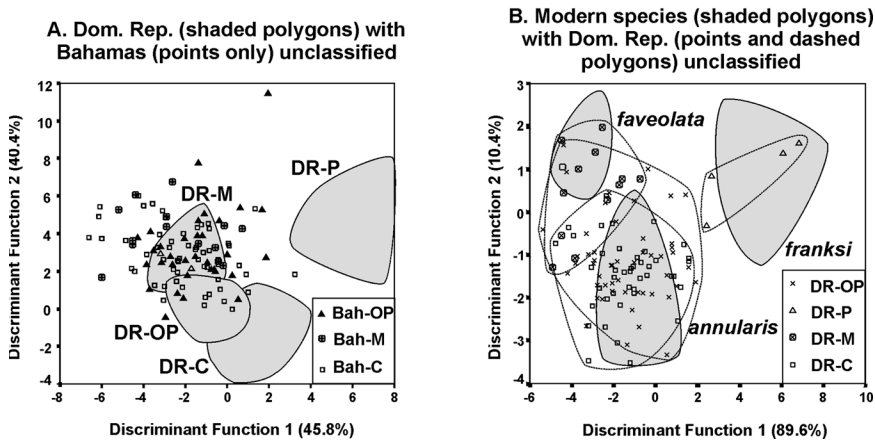


FIGURE 14. Plots of scores in canonical discriminant analyses comparing the four Pleistocene Dominican Republic growth forms with the Pleistocene Bahamas growth forms (A) and the three modern species (B). Each point on the plots represents one colony; polygons enclose growth forms or species. C = columns, M = massive colonies, OP = organ-pipes, P = platy. In both canonical discriminant analyses, wall thickness (x14, x21) is most strongly correlated with the first function; corallite size (csize, LENGTH), in combination with wall structure (y21, y19), is most strongly correlated with the second function. "Unclassified" means that these colonies were not assigned a priori groups when performing the discriminant analyses.

In comparisons with the three modern species (Fig. 14B), the Pleistocene Dominican Republic growth forms more closely match the three Recent Panama species than the Pleistocene Bahamas growth forms do (Fig. 12). Dominican Republic plates overlap and are not statistically significantly different from *M. franksi* ("high" overlap), Dominican Republic massives overlap and are not statistically significantly different from *M. faveolata* ("high" overlap), and Dominican Republic columns overlap and are not statistically significantly different from *M. annularis* s.s. ("high" overlap; see also Klaus and Budd 2003). Dominican Republic organ-pipes overlap and are not statistically significantly different from *M. annularis* ("high" overlap), but they also overlap "moderately" with *M. faveolata* (Fig. 14B). In contrast, the three Bahamas growth forms have more morphologies intermediate between the three modern species (Fig. 12). In particular, the match observed between Dominican Republic massives and *M. faveolata* contrasts with the differences observed between Bahamas massives and *M. faveolata*.

Discussion

Ecology.—The reduction in morphologic distinctiveness observed among species in the Pleistocene of the Bahamas and their high

morphologic variability suggest that ecologic factors, such as competition, may be less effective in maintaining species boundaries in the Bahamas than in the southern Caribbean (described in Pandolfi et al. 2002). Indeed, not only does morphology overlap less among species, but also local distributions overlap less in the southern Caribbean, both today and in the Pleistocene, than in the Pleistocene of the Bahamas. This reduced overlap suggests greater niche differentiation in the southern Caribbean.

Today in Panama, local distributions of the three species within the complex overlap (Knowlton et al. 1992; Weil and Knowlton 1994), but the three species (especially *M. franksi*) differ in the reef zone in which they are most abundant. On protected reefs, the distributions of *M. annularis* s.s. and *M. faveolata* range from 0 to 12 m, with *M. faveolata* being most abundant at 0–3 m and *M. annularis* s.s. being most abundant at 3–6 m. However, on exposed reefs, the distribution of *M. faveolata* extends down to 15 m, with its peak abundance at 3–6 m, as in *M. annularis* s.s. On protected and exposed reefs, *M. franksi* extends from 3 to 24 m and its peak abundance is at 12–15 m. In Curaçao (van Veghel and Bak 1993; van Veghel 1994), the differences in distribution among species are even more pro-

nounced. *M. annularis* s.s. ranges from 3 to 15 m (peak at 6 m), *M. faveolata* from 3 to 25 m (peak at 9 m), and *M. franksi* from 15 to 25 m (peak at 20 m). In the Pleistocene of Curaçao (Pandolfi and Jackson 2001) and Barbados (Pandolfi et al. 2001), species abundances also differ among environments. In the Pleistocene of Curaçao (Pandolfi and Jackson 2001), organ-pipes are most abundant in high- to intermediate-energy environments, columns (= *M. annularis* s.s.) are most abundant in intermediate- to low-energy environments, and massives (= *M. faveolata*) are most abundant in low-energy environments where the other two species were rare or absent. In the Pleistocene of Barbados (Pandolfi et al. 2001), organ-pipes are most abundant in the shallow forereef, and they increase in abundance through geologic time as abundances of columns (*M. annularis* s.s.) decrease. Taken together, these distributions support niche differentiation in the species complex in the southern Caribbean.

In contrast, in the Pleistocene of the Bahamas (this study), species with columnar growth forms are widespread, and differences in local distributions among species are less well defined. In general, organ-pipes prefer patch reef environments and are more abundant there than on the reef crest. Massives have patchy distributions, which appear unrelated to the environment (Fig. 8). This pattern is similar to that observed in the Pleistocene of the Dominican Republic (Klaus and Budd 2003). Although columns are more abundant than other growth forms in all three environments, differentiation among growth forms still occurs, with columns having the highest abundance in the back-reef (low energy), and organ-pipes have highest abundances in the reef front (high energy), in a pattern more like that of the southern Caribbean. Thus, the Bahamas appear unique in the high degree of ecologic overlap and reduced niche differentiation among species.

Morphology.—The observed differences in colony and corallite morphology (Fig. 9) suggest that the three Pleistocene Bahamas growth forms represent species (= distinct evolutionary units), albeit “moderately” overlapping. The observed overlap and fuzzy species boundaries contrast markedly with the structures of species boundaries observed

among modern members of the complex today in Panama (Knowlton et al. 1992; Weil and Knowlton 1994; Budd and Johnson 1996; Budd and Klaus 2001; Knowlton and Budd 2001) and in Curaçao (van Veghel and Bak 1993). At both of these two southern Caribbean locations, morphologies of species are distinct and separated from one another by gaps. Instead, the Pleistocene Bahamian species boundaries more closely resemble those observed today in the Bahamas (Fig. 2).

Our results further suggest that environmental variation alone is not responsible for the morphologic overlap observed among species. Within both columnar and massive forms, much of the difference among reef crest and patch reef environments involves characters that do not differ among species; characters that best distinguish species exhibit little or no environmental variation (Fig. 11, Appendix 5). Thus species overlap primarily involves characters that do not exhibit environmental variation, and appears to have some genetic basis.

Comparisons in space and time suggest that the amount of morphologic overlap among Pleistocene species varies geographically across the Caribbean in much the same way as it does today, with overlap being higher in the Bahamas than in other regions of the Caribbean. However, although less pronounced, morphologic overlap among species does occur at other locations in the Caribbean Pleistocene. For example, even though growth forms in the Pleistocene of the Dominican Republic form more distinct clusters than in the Pleistocene of the Bahamas (Fig. 14), overlap is observed between columns and organ-pipes (instead of between massives and columns as in the Bahamas). Patterns similar to the Dominican Republic are observed in the Pleistocene of Barbados, where corallite morphologies of columns and organ-pipes are distinct and organ-pipes are more similar to modern Panama *M. annularis* s.s. (Pandolfi et al. 2002: Fig. 5).

Hybridization and Reticulate Evolution.—The above comparisons indicate that the observed ecologic and morphologic overlap among species was geographically limited and may have persisted for more than 100,000 years. Our ecologic and morphologic analyses indicate

reduced niche differentiation and “moderate” to “high” morphologic overlap among Pleistocene species, which corroborate the hypothesis of past hybridization and reticulate evolution within the *M. “annularis”* complex. Moreover they indicate that hybridization may have occurred in the Bahamas prior to or during the late Pleistocene, in association with sea level and climatic fluctuations that repeatedly drained and flooded the Bahamas platform.

The observed morphologic intermediacy and lack of distinctiveness of the Bahamas Pleistocene species suggests that hybridization homogenized gene pools and morphologies within the complex (introgressive hybridization), rather than creating morphologically distinct new hybrid species and evolutionary novelties. Previous analyses of Pliocene to Recent occurrences at other locations (Fig. 3) indicate that hybridization involved well-established, preexisting lineages (e.g., *M. annularis* s.s. and *M. faveolata*), which were more speciose prior to high extinction during Plio-Pleistocene time (Budd and Klaus 2001), and resulted in ecologic and morphologic overlap that has persisted until today. Hybridization appears to have resulted in partial lineage fusion; some lineages appear to have merged, whereas others have maintained their differences through time despite overlap. *M. franksi* and *M. annularis* s.s. are genetically indistinguishable today in the Bahamas, and some *M. faveolata* individuals have *M. annularis* s.s.-like genotypes (Fukami et al. 2004).

The observed long-term persistence of overlapping species boundaries and their geographic restriction supports the notion that historical factors, associated with past dispersal events and Pleistocene climate change, have played an important role in shaping the structure of species boundaries on modern-day coral reefs (Pandolfi 1992; Veron 1995; Benzie 1999). Our results differ from those of Vollmer and Palumbi (2002), in which Caribbean-wide hybridization in *Acropora* is interpreted as enhancing morphologic diversity but having little long-term evolutionary influence. In the present case, hybridization was geographically limited and resulted in overlapping, intermediate morphologies and partial lineage fusion. Although the degree of evolutionary influence is not yet known, its ef-

fects appear to have persisted through geologic time. Moreover, our study indicates that the history of hybridization in the complex is traceable in the fossil record by using morphologic data; indeed, in this case, morphology does appear to be linked with the variation in the genotype (but see Miller and Benzie 1997; van Oppen et al. 2001). To further evaluate the hypothesis of persistence, more analyses need to be performed on fossil and living members of the complex in the Bahamas, possibly over a continuous sequence of time intervals extending from Pleistocene to Recent using material in drill cores.

Conclusions

In sum, our study indicates the following about the *M. “annularis”* species complex in the Pleistocene of the Bahama Islands:

1. The local distributions of Pleistocene Bahamian species are broad, extending across reef environments; only organ-pipes exhibit habitat preferences as revealed by higher abundances in patch reef environments. However, these preferences are not as well defined as those observed elsewhere in the Caribbean.
2. Growth forms distinguished in the field (i.e., column, massive, organ-pipe) differ in corallite morphology. Walls are generally thin and septothecal in organ-pipe forms, and costae are short; wall dissepiment and costae are better developed in massive forms. Columnar forms have intermediate wall thicknesses and longer costae. Despite these differences, corallite morphologies of the three growth forms overlap “moderately.” Moreover, spatial distributions of the three growth forms overlap both locally across reef environments and geographically across the Bahamas platform, indicating that the observed morphologic differences are not simply the result of environmental or geographic variation. These results suggest that at least three overlapping species existed within the complex in the Pleistocene of the Bahamas.
3. Analyses of morphologic variation within the Pleistocene Bahamian species indicate that many of the morphologic characters that vary within species do not vary among

- species. The differences among species are not caused by environmental variation.
4. Corallite morphologies of all three Pleistocene Bahamas species (column, massive, organ-pipe) are most similar to modern Panama *M. annularis* s.s. Relative to the three modern Panama species, the Pleistocene species overlap "moderately" and occupy morphospace intermediate between the modern species. In contrast, corallite morphologies of three Pleistocene Dominican Republic species better match their growth form counterparts today in Panama, and exhibit less overlap.
 5. The observed "moderate" species overlap and intermediacy are interpreted as having been caused by past hybridization, which occurred among preexisting lineages in the Bahamas most likely in association with Pleistocene sea level and climate fluctuations. The overlap is important in its limited geographic distribution and apparent long duration in geologic time. Historical factors and past dispersal barriers have had a long-term influence on the morphologic and ecologic distinctiveness as well as the genetic structure of modern-day Bahamian species.

Acknowledgments

We thank N. Knowlton for discussions; B. White, A. Curran, B. Greenstein, C. Carney, M. Boardman, R. Ginsburg, and W. Ausich for locality information; J. Dawson and J. Klaus for assistance in collecting transect data; S. Wallace, J. Wingerath, M. Holcomb, and J. Bean for morphologic measurements; K. Saville and D. Dean for thin-section preparation. We are also grateful to K. Buchan and the Bahamian Field Station (San Salvador), the Forfar Station (Andros), and N. Sealey for assistance with field logistics. This research was supported by a grant from the National Science Foundation (NSF EAR 97-25273) to A.F.B.

Literature Cited

- Benzie, J. A. H. 1999. Genetic structure of coral reef organisms: ghosts of dispersal past. *American Zoologist* 39:131–145.
- Bookstein, F. L. 1991. Morphometric tools for landmark data. Cambridge University Press, Cambridge.
- Bray, J. R., and J. T. Curtis. 1957. An ordination of the upland forest communities of southern Wisconsin. *Ecological Monographs* 27:325–349.
- Budd, A. F. 1993. Variation within and among morphospecies of *Montastraea*. *Courier Forschungsinstitut Senckenberg* 164: 241–254.
- Budd, A. F., and K. G. Johnson. 1996. Recognizing species of Late Cenozoic Scleractinia and their evolutionary patterns. *Paleontological Society Papers* 1:59–79.
- . 1999. Origination preceding extinction during Late Cenozoic turnover of Caribbean reefs. *Paleobiology* 25:188–200.
- Budd, A. F., and J. S. Klaus. 2001. The origin and early evolution of the *Montastraea* "annularis" species complex (Anthozoa: Scleractinia). *Journal of Paleontology* 75:527–545.
- Chen, J. H., H. A. Curran, B. White, and G. J. Wasserburg. 1991. Precise chronology of the last interglacial period: 234U–230Th data from fossil coral reefs in the Bahamas. *Geological Society of America Bulletin* 103:82–97.
- Curran, H. A., and B. White. 1984. Field guide to the Cockburn Town fossil coral reef. Pp. 71–96 in J. W. Teeter, ed. *Proceedings of the second symposium on the geology of the Bahamas*. CCFL Bahamian Field Station, San Salvador, Bahamas.
- . 1985. The Cockburn Town fossil coral reef. Pp. 95–120 in H. A. Curran, ed. *Pleistocene and Holocene carbonate environments on San Salvador Island, Bahamas*. Guidebook for field trip 2, the Geological Society of America annual meeting, Orlando, Florida. Geological Society of America, Boulder, Colo.
- Faith, D. P., P. R. Minchin, and L. Belbin. 1987. Compositional dissimilarity as a robust measure of ecological distance. *Vegetatio* 69:57–68.
- Field, J. G., K. R. Clarke, and D. R. M. Warwick. 1982. A practical strategy for analyzing multispecies distribution patterns. *Marine Ecology Progress Series* 8:37–52.
- Foster, A. B. 1979. Phenotypic plasticity in the reef corals *Montastraea annularis* (Ellis and Solander) and *Siderastrea siderea* (Ellis and Solander). *Journal of Experimental Marine Biology and Ecology* 39:25–54.
- Fukami, H., A. F. Budd, D. R. Levitan, J. Jara, R. Kersanach, and N. Knowlton. 2004. Geographical differences in species boundaries among members of the *Montastraea annularis* complex based on molecular and morphological markers. *Evolution* 58:308–323.
- Graus, R. R., and I. G. Macintyre. 1982. Variation in growth forms of the reef coral *Montastrea annularis* (Ellis and Solander): a quantitative evaluation of growth response to light distribution using computer simulation. In K. Rützler and I. G. Macintyre, eds. *The Atlantic Barrier Reef Ecosystem at Carrie Bow Cay, Belize*, Smithsonian Contributions to the Marine Sciences 12:441–464.
- Harrison, R. G. 1990. Hybrid zones: windows on evolutionary process. *Oxford Surveys in Evolutionary Biology* 7:69–128.
- Hatta, M., H. Fukami, W. Wang, M. Omori, K. Shimoike, T. Hayashibara, Y. Ina, and T. Sugiyama. 1999. Reproductive and genetic evidence for a reticulate evolutionary history of mass spawning corals. *Molecular Biology and Evolution* 16:1607–1613.
- Holcomb, M., J. M. Pandolfi, I. G. Macintyre, and A. F. Budd. In press. Use of X-radiographs to distinguish members of the *Montastraea* "annularis" reef coral species complex. In D. G. Fautin, J. A. Westfall, P. Cartwright, M. Daly, and C. R. Wyttenbach, eds. *Coelenterate biology 2003: trends in research on Cnidaria and Ctenophora*. *Hydrobiologia*.
- Jackson, J.B.C., A. F. Budd, and J. M. Pandolfi. 1996. The shifting balance of natural communities? Pp. 89–122. in D. Jablonski, D. H. Erwin, and J. H. Lipps, eds. *Evolutionary paleobiology: essays in honor of James W. Valentine*. University of Chicago Press, Chicago.
- Klaus, J. S., and A. F. Budd. 2003. Comparison of Caribbean coral reef communities before and after Plio-Pleistocene faunal turnover: analyses of two Dominican Republic reef sequences. *Palaeos* 18:3–21.

- Knowlton, N., and A. F. Budd. 2001. Recognizing coral species past and present. Pp.97–119 in J. B. C. Jackson, S. Lidgard, and F. K. McKinney, eds. *Evolutionary patterns: growth, form, and tempo in the fossil record*. University of Chicago Press, Chicago.
- Knowlton, N., E. Weil, L. A. Weigt, and H. M. Guzman. 1992. Sibling species in *Montastraea annularis*, coral bleaching, and the coral climate record. *Science* 255:330–333.
- Knowlton, N., J. L. Mate, H. M. Guzman, R. Rowan, and J. Jara. 1997. Direct evidence for reproductive isolation among the three species of the *Montastraea annularis* complex in Central America (Panamá and Honduras). *Marine Biology* 127:705–711.
- Lopez, J. V., and N. Knowlton. 1997. Discrimination of sibling species in the *Montastraea annularis* complex using multiple genetic loci. *Proceedings of the Eighth International Coral Reef Symposium* 2:1613–1618.
- Lopez, J. V., R. Kersanach, S. A. Rehner, and N. Knowlton. 1999. Molecular determination of species boundaries in corals: genetic analysis of the *Montastraea annularis* complex using amplified fragment length polymorphism and a microsatellite marker. *Biological Bulletin* 196:80–89.
- Marquez, L. M., M. J. H. van Oppen, B. L. Willis, A. Reyes, and D. J. Miller. 2002. The highly cross-fertile coral species, *Acropora hyacinthus* and *Acropora cytherea*, constitute statistically distinguishable lineages. *Molecular Ecology* 11:1339–1349.
- Miller, K. J., and J. A. H. Benzie. 1997. No clear genetic distinction between morphological species within the coral genus *Platygyra*. *Bulletin of Marine Science* 61:907–917.
- Neumann, A. C., and W. S. Moore. 1975. Sea level events and Pleistocene coral ages in the northern Bahamas. *Quaternary Research* 5:215–224.
- Odorico, D. and D. J. Miller. 1997. Variation in the ribosomal internal transcribed spacers and 5.8S rDNA among five species of *Acropora* (Cnidaria; Scleractinia): patterns of variation consistent with reticulate evolution. *Molecular Biology and Evolution* 14:465–473.
- Pandolfi, J. M. 1996. Limited membership in Pleistocene reef coral assemblages from the Huon Peninsula, Papua New Guinea: constancy during global change. *Paleobiology* 22: 152–176.
- . 2001. Numerical and taxonomic scale of analysis in paleoecological data sets: Examples from Neo-tropical Pleistocene reef coral communities. *Journal of Paleontology* 75:546–563.
- Pandolfi, J. M., and J. B. C. Jackson. 2001. Community structure of Pleistocene coral reefs of Curaçao, Netherlands Antilles. *Ecological Monographs* 71:49–67.
- Pandolfi, J. M., and P. R. Minchin. 1995. A comparison of taxonomic composition and diversity between reef coral life and dead assemblages in Madang Lagoon, Papua New Guinea: Palaeogeography, Palaeoclimatology, Palaeoecology 119:321–341.
- Pandolfi, J. M., J. B. C. Jackson, and J. Geister. 2001. Geologically sudden extinction of two widespread late Pleistocene Caribbean reef corals. Pp.120–158 in J. B. C. Jackson, S. Lidgard, and F. K. McKinney, eds. *Evolutionary patterns: growth, form, and tempo in the fossil record*. University of Chicago Press, Chicago.
- Pandolfi, J. M., C. E. Lovelock, and A. F. Budd. 2002. Character release following extinction in a Caribbean reef coral species complex. *Evolution* 56:479–501.
- Rodriguez-Lanetty, M., and O. Hoegh-Guldberg. 2002. The phylogeography and connectivity of the latitudinally widespread scleractinian coral *Plesiastrea versipora* in the western Pacific. *Molecular Ecology* 11:1177–1189.
- Rowan, R., and N. Knowlton. 1995. Intraspecific diversity and ecological zonation in coral algal symbiosis. *Proceedings of the National Academy of Sciences USA* 92:2850–2853.
- Szmant, A. M., E. Weil, M. W. Miller, and D. E. Colon. 1997. Hybridization within the species complex of the scleractinian coral *Montastraea annularis*. *Marine Biology* 129:561–572.
- Tomaschik, T. 1990. Growth rates of two morphotypes of *Montastraea annularis* along a eutrophication gradient, Barbados, W.I. *Marine Pollution Bulletin* 21:376–380.
- Tomb, J. M. 1995. Description and depositional interpretation of a Pleistocene coral reef, Nichollstown, Andros Island, Bahamas. Unpublished senior thesis. Wright State University, Dayton, Ohio.
- van Oppen, M. J. H., B. L. Willis, J. A. Van Vugt, and D. J. Miller. 2000. Examination of species boundaries in the *Acropora cervicornis* group (Scleractinia, Cnidaria) using nuclear DNA sequence analyses. *Molecular Ecology* 9:1363–1373.
- van Oppen, M. J. H., B. J. McDonald, B. L. Willis, and D. J. Miller. 2001. The evolutionary history of the coral genus *Acropora* (Scleractinia, Cnidaria) based on a mitochondrial and a nuclear marker: reticulation, incomplete lineage sorting, or morphological convergence? *Molecular Biology and Evolution* 18: 1315–1329.
- van Oppen, M. J. H., B. L. Willis, T. van Rheede, and D. J. Miller. 2002. Spawning times, reproductive compatibilities and genetic structuring in the *Acropora aspera* group: evidence for natural hybridization and semi-permeable species boundaries in corals. *Molecular Ecology* 11:1363–1376.
- van Veghel, M. L. J. 1994. Reproductive characteristics of the polymorphic Caribbean reef building coral, *Montastraea annularis*: genetic, behavioral, and morphometric aspects. *Marine Ecology Progress Series* 109:209–219.
- van Veghel, M. L. J., and R. P. M. Bak. 1993. Intraspecific variation of a dominant Caribbean reef building coral, *Montastraea annularis*: genetic, behavioral and morphometric aspects. *Marine Ecology Progress Series* 92:255–265.
- Vaughan, T. W. 1919. Fossil corals from Central America, Cuba, and Porto Rico with an account of the American Tertiary, Pleistocene, and Recent coral reefs. U.S. National Museum Bulletin 103:189–524.
- Veron, J. E. N. 1995. *Corals in space and time*. UNSW Press, Sydney.
- Vollmer, S. V., and S. R. Palumbi. 2002. Hybridization and the evolution of reef coral diversity. *Science* 296:2023–2025.
- Weil, E., and N. Knowlton. 1994. A multi-character analysis of the Caribbean coral *Montastraea annularis* (Ellis and Solander, 1786), and its two sibling species, *M. faveolata* (Ellis and Solander, 1786) and *M. franksi* (Gregory, 1895). *Bulletin of Marine Science* 55:151–175.
- White, B. 1989. Field guide to the Sue Point fossil coral reef, San Salvador Island, Bahamas. Pp. 353–365. in J. E. Mylroie, ed. *Proceedings of the fourth symposium on the geology of the Bahamas*. CCFL Bahamian Field Station, San Salvador, Bahamas.
- White, B., and H. A. Curran. 1987. Coral reef to eolianite transition in the Pleistocene rocks of Great Inagua Island. Pp. 165–179 in H. A. Curran, ed. *Proceedings of the third symposium on the geology of the Bahamas*. CCFL Bahamian Field Station, San Salvador, Bahamas.
- . 1995. Entombment and preservation of Sangamonian coral reefs during glacioeustatic sea-level fall, Great Inagua Island, Bahamas. In H. A. Curran and B. White, eds. *Terrestrial and shallow marine geology of the Bahamas and Bermuda*. Geological Society of America Special Paper 300:51–61.
- White, B. and M. A. Wilson. 1998. Bahamian coral reefs yield evidence of a brief sea-level lowstand during the last interglacial. *Carbonates and Evaporites* 13:10–22.
- Wilson, M. A., H. A. Curran, and B. White. 1998. Paleontological evidence of a brief global sea-level event during the last interglacial. *Lethaia* 31:241–250.

Appendix 1

List of specimens analyzed. Environments (based on GNMDS, Figure 7): 1 = reef crest, 2 = patch reef, 3 = fore-reef. Growth form (based on criteria given in "transects and sampling"); C = columnar, M = massive, OP = organ-pipe.

Environment	Specimen BPK no.	Sample no.	Island	Growth form (field)
3	10022	BP99-11W	Andros	C
3	10045	BP99-11W	Andros	OP
3	10050	BP99-14M	Andros	C
3	10054	BP99-12M	Andros	C
3	10057	BP99-13W	Andros	M
3	10061	BP99-13W	Andros	C
2	10104	BP99-05W	San Salvador	OP
2	10115	BP99-05W	San Salvador	C
2	10141	BP99-25W	Gt. Inagua	OP
1	10142	BP99-15/16M	Gt. Inagua	C
1	10148	BP99-15/16M	Gt. Inagua	M
2	10149	BP99-26M	Gt. Inagua	OP
2	10151	BP99-25W	Gt. Inagua	M
2	10152	BP99-25W	Gt. Inagua	M
2	10153	BP99-25W	Gt. Inagua	OP
2	10154	BP99-26M	Gt. Inagua	OP
2	10157	BP99-18M	Gt. Inagua	M
1	10158	BP99-15/16M	Gt. Inagua	C
1	10159	BP99-15/16M	Gt. Inagua	OP
1	10160	BP99-15/16M	Gt. Inagua	C
1	10166	BP99-15/16M	Gt. Inagua	C
1	10172	BP99-15/16M	Gt. Inagua	C
1	10175	BP99-24M	Gt. Inagua	C
1	10179	BP99-15/16M	Gt. Inagua	C
1	10184	BP99-15/16M	Gt. Inagua	OP
1	10204	BP99-21W	Gt. Inagua	C
1	10205	BP99-22M	Gt. Inagua	M
1	10206	BP99-21W	Gt. Inagua	C
2	10212	BP99-18M	Gt. Inagua	C
2	10215	BP99-25W	Gt. Inagua	C
1	10219	BP99-22M	Gt. Inagua	OP
1	10220	BP99-22M	Gt. Inagua	OP
1	10221	BP99-21W	Gt. Inagua	C
1	10224	BP99-22M	Gt. Inagua	C
2	10225	BP99-25W	Gt. Inagua	C
2	10241	BP99-25W	Gt. Inagua	OP
1	10253	BP99-16M	Gt. Inagua	C
1	10256	BP99-16M	Gt. Inagua	C
1	10258	BP99-16M	Gt. Inagua	M
1	10259	BP99-24M/30-40M	Gt. Inagua	M
1	10260	BP99-24M/30-40M	Gt. Inagua	C
1	10261	BP99-24M/30-40M	Gt. Inagua	M
2	10269	BP99-25W	Gt. Inagua	M
1	10270	BP99-24M/30-40M	Gt. Inagua	C
1	10276	BP99-24M	Gt. Inagua	C
1	10278	BP99-16M	Gt. Inagua	M
1	10279	BP99-16M	Gt. Inagua	C
1	10280	BP99-16M	Gt. Inagua	M
1	10282	BP99-24M	Gt. Inagua	OP
1	10284	BP99-24M	Gt. Inagua	C
1	10285	BP99-24M	Gt. Inagua	C
1	10286	BP99-24M	Gt. Inagua	C
2	10291	BP99-25W	Gt. Inagua	C
2	10292	BP99-25W	Gt. Inagua	C
2	10293	BP99-09W	San Salvador	OP
2	10295	BP99-10M	San Salvador	OP

Appendix 1. Continued.

Environment	Specimen BPK no.	Sample no.	Island	Growth form (field)
2	10307	BP99-09W	San Salvador	C
2	10308	BP99-09W	San Salvador	C
2	10310	BP99-10M	San Salvador	OP
2	10315	BP99-17W	Gt. Inagua	OP
2	10316	BP99-10M	San Salvador	OP
2	10320	BP99-25W	Gt. Inagua	OP
1	10321	BP99-22M	Gt. Inagua	C
1	10328	BP99-22M	Gt. Inagua	C
2	10335	BP99-17W	Gt. Inagua	OP
1	10347	BP99-22M	Gt. Inagua	OP
2	10348	BP99-18M	Gt. Inagua	C
2	10350	BP99-17W	Gt. Inagua	C
2	10352	BP99-17W	Gt. Inagua	C
2	10353	BP99-18M	Gt. Inagua	C
1	10355	BP99-22M	Gt. Inagua	C
2	10356	BP99-17W	Gt. Inagua	OP
2	10360	BP99-26M	Gt. Inagua	OP
2	10371	BP99-26M	Gt. Inagua	C
2	10373	BP99-25W	Gt. Inagua	C
2	10378	BP99-25W	Gt. Inagua	C
1	10379	BP99-22M	Gt. Inagua	C
2	10387	BP99-17W	Gt. Inagua	OP
2	10393	BP99-25W	Gt. Inagua	OP
2	10394	BP99-18M	Gt. Inagua	OP
2	10396	BP99-17W	Gt. Inagua	OP
1	10398	BP99-20M	Gt. Inagua	OP
1	10400	BP99-20M	Gt. Inagua	C
2	10401	BP99-18M	Gt. Inagua	C
2	10403	BP99-25W	Gt. Inagua	C
1	10404	BP99-21W	Gt. Inagua	C
1	10409	BP99-20M	Gt. Inagua	C
2	10410	BP99-25W	Gt. Inagua	C
1	10411	BP99-20M	Gt. Inagua	C
2	10416	BP99-25W	Gt. Inagua	C
2	10419	BP99-17W	Gt. Inagua	OP
1	10421	BP99-16M	Gt. Inagua	C
2	10422	BP99-25W	Gt. Inagua	C
1	10424	BP99-24M	Gt. Inagua	C
1	10429	BP99-24M	Gt. Inagua	OP
2	10431	BP99-09W	San Salvador	C
2	10436	BP99-10M	San Salvador	OP
2	10441	BP99-09W	San Salvador	OP
2	10443	BP99-09W	San Salvador	OP
2	10444	BP99-09W	San Salvador	C
2	10449	BP99-03W/4M	San Salvador	OP
2	10452	BP99-03W/4M	San Salvador	M
2	10455	BP99-03W/4M	San Salvador	M
2	10459	BP99-03W/4M	San Salvador	OP
2	10463	BP99-07W/8M	San Salvador	C
2	10481	BP99-07W/8M	San Salvador	OP

Appendix 2

Transect vs. taxon data matrices analyzed with PRIMER. Values are the summed lengths (m) of transect line intercepted by each species. All transects were 40 m in length.

Species	BP99-3W	BP99-4M	BP99-5W	BP99-6M	BP99-7W	BP99-8M	BP99-9W	BP99-10M	BP99-11W	BP99-12M
<i>Acropora cervicornis</i>	0	0	0.91	0	4.88	0	5.43	0	23.46	0
<i>Acropora palmata</i>	5.78	0	0.69	0	0.15	0	0.37	0	0	0
<i>Agaricia agaricites</i>	0	0	0	0	0	0	0	0	0	0
<i>Siderastrea radians</i>	0	0	0	0	0	0	0	0	0.08	0
<i>Siderastrea siderea</i>	0	0	0.19	0	0.5	0	0	0	1.22	0
<i>Porites asteroides</i>	0	0	1.3	0	1.07	0	0.68	0	0	0
<i>Porites furcata</i>	2.43	0	0	0	0	0	0.32	0	0	0
<i>Favia fragum</i>	0	0	0	0	0	0	0	0	0	0
<i>Diploria clivosa</i>	0	0	0	0	0	0	0	0	0	0
<i>Diploria labyrinthiformis</i>	0	0	1.23	0	1.43	0	0.33	0	0.36	0
<i>Diploria strigosa</i>	2.82	0	2.46	0	0	0	0.66	0	1.43	0
<i>Manicina areolata</i>	0	0	0.23	0	0	0	0	0	0	0
Columnar <i>Montastraea</i>	0	0	1.34	1.43	11.73	14.74	5.52	6.72	1	1.37
Massive <i>Montastraea</i>	4.3	5.31	1.43	0	0.32	1.63	0	0	0	0
Platy <i>Montastraea</i>	0	0	0	0	0	0	0.73	0	0	0
<i>Montastraea cavernosa</i>	0	0	0	0	0.46	0	0	0	0	0
Organ-pipe <i>Montastraea</i>	8.95	13.82	10.29	11.11	9.1	9.36	12.37	16.9	4.9	5.32
<i>Dichocoenia stokesi</i>	0	0	0	0	0.15	0	0	0	0	0
<i>Isophyllastrea rigida</i>	0	0	0	0	0	0	0	0	0	0
<i>Eusmilia fastigiata</i>	0	0	0	0	0	0	0	0	0.14	0
<i>Isophyllia sinuosa</i>	0	0	0	0	0	0	0	0	0	0
? <i>Mussismilia</i> sp.	0	0	0	0	0	0	0	0	0	0
Total coral recorded	24.28	19.13	20.07	12.54	29.79	25.73	26.41	23.62	32.59	6.69

Appendix 2. Extended.

BP99-13W	BP99-14M	BP99-15W	BP99-16M	BP99-17W	BP99-18M	BP99-19W	BP99-20M	BP99-21W	BP99-22M	BP99-23W	BP99-24M	BP99-25W	BP99-26M
17.125	0	6.45	0	3.11	0	0.7	0	0.58	0	10.31	0	0.1	0
0	0	4.77	0	3.64	0	10.82	0	12.6	0	6.14	0	0	0
0	0	7.43	0	0.25	0	8.73	0	0	0	0.41	0	0	0
0	0	0	0	0	0	0	0	0	0	0	0	0	0
0	0	0	0	0	0	0	0	0	0	0	0	0	0
0	0	0.14	0	0.26	0	0	0	0.06	0	0.06	0	0	0
0	0	0.26	0	0.31	0	0	0	0	0	0.58	0	0	0
0	0	0	0	0.15	0	0	0	0	0	0	0	0	0
0.3	0	0.55	0	0.61	0	0	0	2.98	0	2.45	0	0	0
0	0	0	0	0.12	0	0	0	0.4	0	0	0	0	0
2.375	0	6.82	0	2.77	0	4.86	0	0.18	0	0.48	0	1.3	0
0	0	0	0	0.05	0	0	0	0	0	0	0	0	0
0.2	0.35	2.92	12.03	4.22	7.6	3.22	6.95	2.95	6.85	0.78	9.62	10.35	17.66
0.95	3.8	0	2.17	0	1.42	0.97	0.54	0	1.19	3.02	4.13	2.22	2.87
0	0	0	0	0	0	0	0	0	0.3	0	0	0	0
0	0	0	0	0.14	0	0	0	0.08	0	0	0	0	0
0	0	1.84	5.45	5.75	9.74	2.1	2.25	0.23	2.54	2.4	2.01	14.05	16.01
0	0	0.1	0	0	0	0	0	0	0	0.1	0	0	0
0.05	0	0.08	0	0	0	0	0	0	0	0.05	0	0	0
0	0	0	0	0	0	0	0	0	0	0	0	0	0
0.15	0	0	0	0	0	0	0	0	0	0	0	0	0
0	0	0	0	0	0	0	0	0	0.22	0	0	0	0
21.15	4.15	31.36	19.65	21.38	18.76	31.4	9.74	20.06	11.1	26.78	15.76	28.02	36.54

Appendix 3

Landmarks on transverse thin-sections of corallites of *Montastraea*. Types: 1 = juxtaposition of structures, 2 = maxima of curvature, 3 = extremal points.

Number	Type	Description
1	3	Center of corallite
2	3	Outermost point on secondary costa
3	1	Outer left junction of secondary costoseptum with wall dissepiment
4	1	Outer right junction of secondary costoseptum with wall dissepiment
5	1	Inner left junction of secondary costoseptum with wall dissepiment
6	1	Inner right junction of secondary costoseptum with wall dissepiment
7	2	Left point of maximum curvature associated with secondary septal thinning
8	2	Right point of maximum curvature associated with secondary septal thinning
9	3	Innermost point on secondary septum
10	3	Outermost point on tertiary costa
11	1	Outer left junction of tertiary costoseptum with wall dissepiment
12	1	Outer right junction of tertiary costoseptum with wall dissepiment
13	1	Inner left junction of tertiary costoseptum with wall dissepiment
14	1	Inner right junction of tertiary costoseptum with wall dissepiment
15	2	Left point of maximum curvature associated with tertiary septal thinning
16	2	Right point of maximum curvature associated with tertiary septal thinning
17	3	Innermost point on tertiary septum
18	3	Outermost point on primary costa
19	1	Outer left junction of primary costoseptum with wall dissepiment
20	1	Outer right junction of primary costoseptum with wall dissepiment
21	1	Inner left junction of primary costoseptum with wall dissepiment
22	1	Inner right junction of primary costoseptum with wall dissepiment
23	2	Left point of maximum curvature associated with primary septal thinning
24	2	Right point of maximum curvature associated with primary septal thinning
25	3	Innermost point on primary septum
26	1	Outer left junction of tertiary costoseptum with wall dissepiment
27	1	Inner left junction of tertiary costoseptum with wall dissepiment

Appendix 4

Correlations between characters (Table 2) and canonical discriminant functions calculated in analyses comparing the three Pleistocene species. * = relatively high correlation.

Character	Environment 1 Reef crest				Environment 2 Patch reef				All 3 Environments			
	Discriminant Function		Character		Discriminant Function		Character		Discriminant Function		Character	
	1	2	1	2	1	2	1	2	1	2	1	2
x2	-0.42006*	-0.22192	y19	0.52112*	-0.22527	ens	-0.46182*	0.18000				
x10	-0.28262*	-0.07293	cd	0.46220*	-0.04637	x10	0.34046*	-0.04616				
x18	-0.21920*	-0.16692	y21	0.40244*	-0.35465	x16	0.31082*	-0.07978				
y22	0.11632	0.02270	LENGTH	0.38134*	-0.23604	CSIZE	-0.24825*	-0.09455				
ens	-0.11125	-0.03571	ens	0.37152*	0.01289	cl	-0.22261*	0.12419				
LENGTH	0.07108	-0.05035	x14	0.32443*	0.07564	x25	0.14329	-0.05603				
tt	-0.05147	-0.01607	y11	0.32405*	-0.08357	tt	-0.13362	0.03687				
cl	0.05036	-0.04902	x21	0.31453*	0.09124	x9	0.11369	-0.02081				
x21	-0.20835	-0.47954*	y22	-0.28921*	0.13674	x17	-0.04988	0.01349				
x14	-0.19250	-0.47111*	x2	0.09608	-0.03352	y19	-0.29782	0.59827*				
y19	-0.07206	-0.45999*	ens	0.18767	-0.43338*	x14	0.00160	0.58767*				
y21	-0.03257	-0.34784*	x18	0.12389	0.35133*	x21	0.01912	0.58044*				
y11	-0.14543	-0.27386*	x10	-0.21265	0.25916*	cd	-0.14397	0.47035*				
x25	0.07321	0.25728*	CSIZE	0.08387	-0.23444*	y21	-0.34131	0.42657*				
td	0.01395	-0.18295	x16	-0.17584	0.20057*	y11	-0.05606	0.42317*				
CSIZE	0.17564	0.18285	x25	0.11835	0.19078	ens	0.04533	0.35171*				
x16	-0.11802	0.17595	x17	0.09114	0.14289	y22	-0.02472	-0.34292*				
x9	0.03429	0.15663	cl	0.07229	-0.12321	LENGTH	-0.26983	0.30694*				
ens	0.06600	-0.10883	x9	0.01271	0.11997	x18	0.23298	0.29214*				
x17	0.01046	-0.07999	td	0.02231	0.08931	x2	0.16898	0.26269*				
cd	0.04329	-0.05017	tt	0.04161	-0.05673	td	-0.13578	0.23121*				

Appendix 5

Correlations between characters (Table 2) and canonical discriminant functions calculated in analyses comparing environments within the three Pleistocene species. * = relatively high correlation.

Columns		Massives		Organ-pipes	
Character	Discriminant function	Character	Discriminant function	Character	Discriminant function
x17	-0.342*	cl	0.478*	x2	0.536*
y22	-0.191	exs	-0.285*	x10	0.257*
ens	0.177	ens	-0.183	x25	-0.227*
x16	0.150	SIZE	0.168	x18	0.219*
x10	0.128	x25	-0.164	y19	0.218*
exs	-0.123	y22	-0.161	cd	-0.195
x25	-0.110	td	0.119	y11	0.183
tt	-0.105	y21	-0.113	tt	0.138
x18	-0.095	x16	-0.110	x14	0.127
cl	0.093	LENGTH	0.106	x21	0.127
x2	0.076	tt	-0.084	SIZE	-0.124
y21	0.066	x2	0.082	LENGTH	-0.122
LENGTH	-0.058	x10	-0.074	x9	-0.097
y11	-0.057	y11	0.053	y21	0.094
SIZE	-0.044	x18	-0.046	cl	-0.076
x9	-0.041	cd	0.045	x17	0.073
y19	-0.024	x21	-0.020	ens	-0.061
td	0.021	x14	-0.019	exs	0.040
x14	0.018	y19	0.015	x16	0.031
x21	0.016	x17	0.012	td	-0.018
cd	0.011	x9	0.002	y22	0.014